Victoria M. Petrova
Editor

Volume 50

# Advances in Engineering Research

NOVA

# Advances in Engineering Research

# Advances in Engineering Research

**Advances in Engineering Research. Volume 49**
Victoria M. Petrova (Editor)
2022. ISBN: 979-8-88697-132-3 (Hardcover)
2022. ISBN: 979-8-88697-156-9 (eBook)

**Advances in Engineering Research. Volume 48**
Victoria M. Petrova (Editor)
2022. ISBN: 978-1-68507-894-2 (Hardcover)
2022. ISBN: 979-8-88697-083-8 (eBook)

**Advances in Engineering Research. Volume 47**
Victoria M. Petrova (Editor)
2022. ISBN: 978-1-68507-796-9 (Hardcover)
2022. ISBN: 978-1-68507-902-4 (eBook)

**Advances in Engineering Research. Volume 46**
Victoria M. Petrova (Editor)
2021. ISBN: 978-1-68507-406-7 (Hardcover)
2021. ISBN: 978-1-68507-427-2 (eBook)

**Advances in Engineering Research. Volume 45**
Victoria M. Petrova (Editor)
2021. ISBN: 978-1-68507-360-2 (Hardcover)
2021. ISBN: 978-1-68507-384-8 (eBook)

**Advances in Engineering Research. Volume 44**
Victoria M. Petrova (Editor)
2021. ISBN: 978-1-53619-950-5 (Hardcover)
2021. ISBN: 978-1-53619-992-5 (eBook)

More information about this series can be found at
https://novapublishers.com/product-category/series/advances-in-engineering-research/

**Victoria M. Petrova**
Editor

# Advances in Engineering Research

**Volume 50**

nova
science publishers
www.novapublishers.com

**Library of Congress Cataloging-in-Publication Data**

ISBN: 979-8-88697-353-2(eBook)
ISSN: 2159-4961

*Published by Nova Science Publishers, Inc. † New York*

# Contents

# Chapter 5

# The Effect of Noise on Dynamics of Natural Processes: A Review of Methodology and Engineering Applications

**Srđan Kostić[1,*], PhD, Nebojša Vasović[2], PhD and Kristina Todorović[3], PhD**

[1]Jaroslav Černi Water Institute, Belgrade, Serbia
[2]University of Belgrade Faculty of Mining and Geology, Belgrade, Serbia
[3]University of Belgrade Faculty of Pharmacy, Belgrade, Serbia

## Abstract

Noise represents a regular companion of almost all natural processes, including earthquakes, landslides and similar, and it exists permanently unrelated to the activity of contemporary geodynamical processes. For example, background seismic noise is recorded regardless of the seismic activity within the monitoring area. However, during the seismic event, noise is also the constituent part of the recorded signal, and it is commonly isolated by applying different processing techniques, i.e., different types of filtering. From the purely theoretical viewpoint, one could single out two major types of noise: random (white) and colored (correlated) noise, with the white noise as the most common type of noise in natural processes. In general, regardless of the type of noise, its main characteristics are extremely small amplitude and high frequency. In most of the cases, due to its small amplitude, noise does not have any significant effect on the triggering, duration and properties of the main event, e.g., landslide movement or seismic fault displacement. Nevertheless, there are certain scenarios when noise could have a crucial

* Corresponding Author's Email: srdjan.kostic@jcerni.rs.

In: Advances in Engineering Research. Volume 50
Editor: Victoria M. Petrova
ISBN: 979-8-88697-283-2

role in the initiation of the instability and its further qualitative properties. Focus on these scenarios is presented in this chapter. After providing theoretical framework on the noise and methods of nonlinear dynamics used to study the noise, i.e., the mean-field approximation in the first place, the largest part of the chapter is concentrated on the influence of different types of noise on the triggering of earthquake fault movement and groundwater level dynamics. Four illustrative examples are studied in detail: effect of the white background noise and impact of the colored noise on the earthquake nucleation, the correlated noise as the constituent part of the model of groundwater level dynamics and the effect of noise on the dynamics of excitable systems. Existence of noise in all three examined cases is firstly proved for the real-world examples, i.e., for the recorded natural signals. In case of earthquake nucleation, it is shown that when stress accumulation along the fault reaches critical values (near the bifurcation) even small-amplitude oscillations (background seismic noise) could be sufficient for triggering the instability. On the other hand, when it comes to the influence of colored noise, it is shown that the increase of correlation time and coupling strength prevents the onset of seismic fault motion, indicating the predominant effect of random (white) seismic noise. Regarding the groundwater level dynamics, results presented in this chapter indicate that only models with the included colored noise could realistically mimic the real groundwater level oscillations. As for the excitable systems, we analyze conditions for which the influence of noise triggers the activation process.

**Keywords**: mean-field approximation, random and colored noise, earthquake, groundwater level dynamics, slope stability, excitability, bifurcation

## Introduction

In geological engineering sciences, role of noise is rarely examined, mostly because its amplitude is significantly smaller compared to the amplitude of the observed process itself, so its effect is considered to be negligible. Also, frequency of natural noise is much higher that the frequency of the process itself, so the changes in event periodicity under the influence of natural noise are also not expected. As addition, for a long time recording instruments were not able to record these phenomena due to relatively high registration threhold. However, in the last two decades, instruments for seismic recordings are being made sensitive enoguh to capture the continuous background vibrations existing permanently between earthquake events. However, results of theoretical considerations, especially in the area of nonlinear dynamics,

showed that effect of noise could be crucial for dynamical systems which are at the verge of stability. In engineering terms, this means that natural processes, such as landslides and earthquakes, when brought to the stability limits due to effect of other factors (such as precipitation, groundwater and surface water level oscillation, soil deformation processes, tectonic movements, etc.), exhibit strong sensitivity to the impact of background noise.

According to Campillo (Nakata et al., 2019) the term "noise" is used to denote weak permanent vibrations in microseism band (0.04-0.2 Hz) produced by seismic waves, although their sources are often poorly understood. Results of the research so far have shown that noise sources are mutiple, resulting from complex processes. Due to sophisticated recording techniques, aquisition and post-processing methods properties of background noise are well known today. Ambient noise wavefield is investigated from the available large sensor arrays, with the possibility to locate the noise sources.

Main properties of this background radiation of Earth (historically referred to as microseisms) are the permanent presence, quasi-randomness and variable amplitude depending on the position, time and frequency. According to Nakata et al., (2019) the absence of an easily identifiable, deterministic signal has led to the common classification of the ambient field as ambient noise.

In particular, according to Webb (2002), there are three main types of natural background noise: long-period noise (<0.1 Hz), short-period noise and microseism peak (0.1 – 0.5 Hz). Class of long-period noise contains: earth tides and low-frequency waves (0.01mHz – 0.1Hz), atmospheric pressure variations, winds and currents, tilt noise (0.2 – 50 mHz), single-frequency microseism peak (0.05 – 1 Hz), surface waves and long-period body waves. Class of short-period noise (> 0.5 Hz) includes short-period band (0.5 – 10 Hz) – microseisms, short-period noise (0.5 – 50 Hz) – land, short-period noise (0.5 – 50 Hz) – sea floor and short-period body waves. Apart from this, some authors identify ship wakes (McNamara et al., 2011) or even rugby matches (Boese et al., 2015) as possible noise sources.

Earth tides represent deformation of the Earth under ocean waves and atmospheric pressure fluctuations, which are commonly observed with long-period seismometers and tiltmeters for many years. This type of tides occurs due to the effect of three main factors: (1) gravitational attraction of the Sun and Moon, (2) gravity variation due to changes in the distance to the center of the Earth from deformation, (3) direct impact of tidal forces. Recordings made near coastlines or at the sea floor are also affected by ocean tides, which is also under the influence of the three main factors: (1) gravitational attraction

of a changing mass of sea water adjacent to oro overhead of a site, (2) variation in apparent gravity due to deformation under the time-varyinf load of sea water, (3) acceleration due directly to this deformation.

Ground noise on land at very long period (0.2 – 50 mHz) is usually associated with atmospheric pressure fluctuations. According to Murphy and Savino (1975), mass of the atmosphere changes with the atmospheric pressure, which further induces changes in gravity which are recorded by vertical component seismometers. Moreover, turbulence in the boundary layer induces fluctuating pressures and ground deformation. At shorter periods, significant deformation to depths of few tens of meters below the ground surface could be caused by turbulence in the atmospheric boundary layer, which in turn produces pressure fluctuations at the Earth's surface. Ocean currents could also form a turbulent boundary layer with advecting pressure fluctuations (Webb, 1988).

Single-frequency microseism peak, according to Webb (2002) occurs as a small peak in the spectrum between 0.05 and 0.1 Hz, and it is directly associated with ocean waves. This peak is called the single-freuqency peak since it represents the swell freuqencies without the frequency doubling observed for the main micro-seism peak. Amplitude of these peaks are much larger at coastal sites than observed either in the center of continents or on the deep ocean floor, where microseism peak is related to storm waves on remote coastlines (Cessaro, 1994).

The microseism peak (0.1-0.5 Hz) commonly represents the reuslt of energetic ocean waves with 10-18s period. In general, ocean waves couple into ground motion as local and the one which travel throughout the Earth.

Short-period band microseisms commonly occur at see floor and could also be associated with breaking waves. On land, these microseisms occur along the coastlines, affected by ocean waves or storm waves on nearby large lakes (Webb, 2002).

Short-period noise (0.5 – 50 Hz) on land is primarily caused by wind and cultural noise with the possible contribution from water movement. At some sites, one could easily spot the seasonal cycle in noise due to wind variations or water flow in nearby rivers. According to McNamara and Boaz (2019) this type of noise propagates mainly as short-period surface waves (0.1-1s) which attenuate several kilometers in distance and depth. Culutral noise is usually associated with the man or man-made machinery: power plants, factories, trains and highways, even diesel generators, water pumps and cattle, but could be ascibed also to natural causes, such as glacier calving and wind. Effect of cultural noise could be avoided by placing the recording instrument at a

sufficient distance from the source: 25km from power plants or rock-crushing machinery, 15km from railways, 6km from highway and more than 1km from smaller roads (Wilmore, 1979). Amplitudes and frequencies of cultural noise could significantly vary between distant sites. Also, one could easily find the differences in cultural noise level for different parts of the day and seasons of the year. For example, according to Fyen (1990), noise levels are the lowest in the early morining rising rapidly near 07:00 to levels sustained during the working day, to fall gradually through the evening hours. On the other hand, noise levels are low during the weekends but increase during the holidays.

According to Campillo (2019) background or ambient noise provides excellent opportunity to repeat measurements of noise at different dates, which emables detection of very small changes in the elastic properties of rock at depth. This could further enable one to capture the small precursory changes of volcanic eruptions, landslides and earthquakes.

In present chapter, we observe the effect of natural background (seismic) noise on the possible earthquake nucleation and noise as the constituent part of groundwater level dynamics. In both cases, significant variation in noise amplitude and frequency is not examined, but it is considered that frequency is significantly higher than the observed process, while noise amplitude is assumed to be significantly smaller thatn the fault movement or groundwater level oscillation. The main focus is on the degree of noise correlation: both random noise (white noise) and correlated noise (colored noise) is analyzed, which is considered significant from the engineering viewpoint. In particular, we consider background seismic noise to be random in case this noise is observed as a product of different natural sources, both cultural and natural. When only a single noise source is assumed, than effect of random noise is analyzed. Moreover, today the seismic ambient field is known to be coherent over length scales (Nakata et al., 2019) and is used constructively in applications ranging from volcano and reservoir monitoring to global seismic tomography. One should note that both coherent and incoherent nature of the seismic noise is confirmed by the analysis of real observed fault movements.

In case of earthquake nucleation, effect of noise is examined for the scenario when the system under study is near the verge of stability, i.e., near the bifurcation curve. Our starting hypothesis is that fault displacement is the most sensitive to the effect of noise at the verge of stability, when even small background variations could be sufficient to trigger the instability. For this purpose, we analyze the spring-block model originally proposed by Burridge and Knopoff (1967), with the following set-up: an array of blocks is interconnected and moving along the rough surface at some constant

beckground velocity. Specific friction laws are assumed to be valid at the contact of blocks and rough surface, while state variable is treated by assuming the effect of time delay in the movement of the blocks.

In general, up until our pioneer work (Vasović et al., 2016) dynamics of spring-block model has been examined without the stochastic effect, which is in fact observed in nature, and commonly originates from heterogenic conditions along the seismogenic fault (Telford et al., 1990; Ryabov et al., 2003). Apart from the analysis of the effect of random noise, we also examine the influence of colored noise, which could be the product of many potential sources (Kostić et al., 2020): reservoir charging/discharging, penetration of sound waves emitted by neighboring fault motion, close earthquakes or explosion, ocean waves and tides, etc., or as the product of pre-processing of the acquired measurements. Regarding the role of noise in groundwater level dynamics, we analyze noise as the consistuve part of the groundwater level oscillation time series, with the aim to explicitly include it in formulating the appropriate estimation models. Model for groundwater level dynamics is defined based on the analysis of real recordings made at several locations in Serbia.

Besides the analysis of the effect of noise on dynamics of the aforementioned natural systems, special attention is devoted to the methods for the analysis of dynamics of stochastic systems, i.e., the justification of the mean-field approximation, which was originally proposed in one of our previous works (Burić et al., 2010). We also elaborate on the conditions for which the application of such method is justified.

The chapter is organized as follows. Section 2 is devoted to the general description of noise from the theoretical vewipoint. In Section 3, we present the mean-field approach for the analysis of stochastic delay differential equations, with included time delay and random/colored noise, with special attention to conditions for which the mean-field approach is valid or fails. In Section 4 we examine the impact of random and colored noise on the seismogenic fault motion. Random noise is particularly examined for cases of global coupling and with varying interaction among the units in the system. For each analyzed instance, appropriate corroboration from the seismological viewpoint is provided. In Section 5 we examine the existence of noise in grondwater level dynamics, with the suggestion of a prediction model with the incorporated effect of noise.

## General on Noise

The influence of noise on nonlinear dynamical systms could be considered as permanent, considering the fact that all natural and non-natural systems evolve in the presence of noisy driving forces. For a long time, noise has been considered to have a blurring effect on the evolution of dynamical systems. Although this could be the case for "observational" or "measurement" noise, including linear systems, in nonlinear systems impact of noise could drastically modify the deterministic dynamics, i.e., it could lead to noise-induced bifurcations. Eventually, influence of noise could cause dynamics of the observed nonlinear system that could be easily mistaken for deterministic chaos, especially in the vicinity of bifurcation points, where noise could have the predominant effect. In excitable processes, for instance, noise connected with the existence of thresholds, separatrices and saddles in dynamical systems, these instable barriers could be passed with finite probability. Here purely noise-idncued processes are excited, which is absent in deterministic model.

From the mathematical standpoint, noise as a random variable is a quantity that fluctuates aperiodically in time. In order to be able to define noise as a useful quantitxy, this random variable needs to have well-defined properties that can be measured experimentally, such as distribution of values (density) with a mean and other moments, and a two-point correlation function. Thus, although the variable itself takes on a different set of values each time we look at it or simulate the process which generates noise (i.e., for each of its realizations) its statistical and temporal properties remain constant. The validity of these assumptions in a particular experimental setting must be properly addressed, for example by verifying that certain stationarity ciretria are satisfied.

The main difficulty with noise modelling is that one commonly does not have access to the noise variable itself. Instead, one commonly has access to a state variable of a system that is perturbed by one or multiple sources of noise. Therefore, one needs to begin with the assumptions on noise and its coupling to the dynamical state variables. The accuracy of these assumptions can later be assessed by looking at the alignment of the predictions of the resulting model with the experimental data.

In case of observational noise, although dynamical system evolves deterministically, measurement recordings are contaminated by noise. For instance, let us suppose a one-dimensional dynamical system, governed by $dx/dt = f(x,\mu)$, where μ is the parameter. In that case, observational noise

corresponds to the measurement of $y = x(t)+\xi(t)$, where $\xi(t)$ is the observational noise process. The measurement y, but not the evolution of the system, is affected by the presence of noise.

Besides this observational noise, one could observe dynamical systems characterized by noise that is independent of the state of the system: $dx/dt = f(x,\mu)+\xi(t)$, where noise is simply added to the deterministic part of dynamics (the so-called additive noise). Also, one could encounter multiplicative noise, when the noise is dependent on the values of one or many state variables. If we suppose that $f$ is separable into deterministic part and stochastic part that depends on x: $dx/dt = h(x) + g(x)\ \xi(t)$, the effect of noise term will depend on the value of the state variable through $g(x)$.

Modelling the precise effects of noise on a dynamical system can be difficult; however, one can already gain insight into the effect of noise on a system by coupling it additively to Gaussian white noise, which is a mathematical construct that approximates the properties of many kinds of noise encountered in experimental situations. Such noise has Gaussian distribution with zero mean and autocorrelation $\langle \xi(t)\xi(s)\rangle = 2D\delta(t-s)$, where δ is the Dirac delta function. The quantity $D = \sigma^2/s$ is usually referred to as the intensity of the Gaussian white noise (the actual intensity with the autocorrelation scaling used in our exampled is $2D$). Strictly speaking, the variance of this noise is infinite, since it is equal to the autocorrelation at zero lag (i.e., at $t = s$). However, its intensity is finite, and σ time s the square root of the time step will be the standard deviation of Gaussian random numbers used to numerically generate such noise.

The Langevin equation referes to the stochastic differential equation obtained by adding Gaussian white noise to a simple first-order linear dynamical system with a single stable fixed point: $dx/dt = -\alpha x+\xi(t)$. The stochastic process $x(t)$ is also known as Ornstein-Uhlenbeck noise with correlation time 1/α, or as lowpass-filtered Gaussian white noise. A noise process that does not have a delta-function autocorrelated is known as colored noise. Therefore, the experimentally correlated Ornstein-Uhlenbeck process is a colored noise. The probability density of this process is given by a Gaussian with zero mean and variance $\sigma^2/2\alpha$. In practical work, it is important to distinguish between this variance and the intensity D of the Gaussian white noise process used to produce it. It is in fact common to plot various quantities of interest for a stochastic dynamical system as a function of the intensity D of the white noise used in that dynamical system, no matter where it appears in equations.

The case in which deterministic part is nonlinear yields a nonlinear Langevin equation. One can simulate a nonlinear Langevin equation with deterministic flow $h(x,t,\mu)$, and a coefficient $g(x,t,\mu)$ for the noise process using various stochastic numerical integration methods of different orders of precision. For instance, one can use a simple stochastic Euler-Maruyama method with fixed time step $\Delta t$ (stochastic simulations are much softer with fixed step methods). Using the definition of Gaussian white noise $\xi$ (t) as the derivation of the Wiener process W(t) (Wiener process is also known as Braunian motion), this method can be written as: $x(t+\Delta t) = x(t)+\Delta t h(x,t,\mu)+g(x,t,\mu)\Delta W_h$, where $\{\Delta W_n\}$ are increments of the Wiener process. These increments can be shown to be independent Gaussian random variables with zero mean and standard deivation given by $\sigma(\Delta t)^{1/2}$. Because the Gaussian white noise is a function that is not differentiable, one must use another kind of calculus to deal with it, like stochastic calculus. In such case, one needs to be cautious when performing a nonlinear change of variables on stochastic differential equations: "The Stratonovich" stochastic calculus obeys the laws of the usual determinsitic calculus, but the "Ito" stochastic calculus does not. Therefore, one has to associate an Ito or Stratonovich interpretation to a stochastic differential equation before performing coordinate changes. Also, for a given stochastic differential equation, the properties of the random process $x(t)$ such as its moment will depend on the choise of cauclus used. Fortunately, there is a simple transfomration between the Ito and Stratonovich forms of thestochastic differential equation. Moreover, properties obtained with both calculi are indentical when noise is additive. It is also important to associate the chosen calculus with a proper integration method. For instance, an explicit Euler-Maruyama scheme is an Ito method, so numerical results with this method will agree with any theoretical results obtained from an analysis of the ito interpretation of the stochastic differential equation, or of its equivalent Strtonovich form. In general, the Stratonovich form is the best choice for modelling the real colored noise and its effect in the limit of vanishing correlation time, i.e., in the limit where colored noise is allowed to become white after the calculation of measurable quantities.

## Mean-Field Approximation

A cumulant approach, together with a Gaussian approximation, allows one to analyze the behavior of an ensemble of coupled elements driven by additive noise. The use of a full set of cumulants or moments instead of hierarchy of

probabilitiy densities is an alternative way to describe a stochastic process (Gardiner, 1985).

For diffusion stochastic processes, the cumulant approach aims to study the dynamics of cumulants, and allows one to analyze a set of ordinary differential equations instead of parabolic partial differential equations (the Fokker-Planck equation). The noise intensity appears to be an additional parameter in cumulant equations. A problem arises, though, when the original stochastic differential equations are nonlinear. In such case, the set of ordinary differential equations for cumulants appears to be unclosed: an equation for the nth order cumulant may contain higher order cumulants. Several approximations can be used to truncate the series of cumulant equations, the simplest one being the Gaussian approximation, which taken into account the evolution of only the first-order and second-order cumulants. The resulting systm of cumulant equations in the Gaussian approximation allows one to perform a bifurcation analysiswith an additional control parameter, namely the noise intensity. The cumulant approach within the Gaussian approximation was successfully used to study the influence of noise on bifurcations in different dynamical systems.

One should note that currently there is no formalism to exactly compute the effects of noise in nonlinear systems with delays. The standard Fokker-Planck approach is not justified since it is meant for Markovian systems. Delay-differential systems are not Markovian, although their various apporoximations might be Markovian. For instance, if the delay is small in comparison with all other time scales of the systm, one can approximate the stochastic delay differential equations by a system of ordinary stochastic differential equations. A notable exception is the class of linear stochastic differential equations with additive noise. In this case, while there is no Fokker-Planck formalism, the statistics of the system are Gaussian and one needs only to compute the first two moments of the probability density of the variable.

## General on Delay and Delay Differential Equations

Delay differential equations occur in a wide variety of the natural and man-made systems. They often arise from an approximation to a partial differential equation that describes for instance diffusion of some reacting substance or a traveling wave in some medium. Delay differential equations are infinite-dimensional dynamical systems: an infinite number of initial conditions – a

function of the initial delay interval – is needed to uniquely specify their time evolution.

Delay differential equations occur also in a variety of applications and the influence of noise on such equations is increasingly in the focus of scientific research. For instance, in laser physics delays arise from finite propagation times inside optical cavities and around optical circuits external to the laser, as well as in optical fiber networks. There are also studies on the enhancement by noise of the oscillations in a network of delayed-coupled oscillators, stochastic resonance in a non-Markovian system and of control of noise induced motion in relaxation oscillators using delayed feedback.

In the biological systems, delays arise from the finite maturation or division time of various cellular species, such as blood cell lines, or the synthesis of various molecular species, as in the immunological system or genetic control systems. In neuroscience, delays arise from the propagation time of nerve impulses across synapses. In such systems, one often faces with the problem of distribution of delays.

In geology, especially in the area on earthquakes and landslides research, existence of delay, although indicated by many previous investigation, as the constituent part of the friction term (state variable) or describing the interaction between neighboring and distance units and/or blocks, has not been studied in detail, especially concerning its significance for engineering practice.

Delay has an important role in the dynamics of the coupled oscillator system, where delay simulates the situation in real-life systems where the interaction between individual oscillators may not be instantaneous but may be delayed due to finite propagation time of signals. Time delays could similarly occur in chemical systems due to finite reaction times, and in biological systems, like neuron assemblies the synaptic integration mechanisms may provide a natural delay. From a mathematical point of view, one can expect time delays to have a profound effect on the dynamical characteristics of a single oscillator. This is well- known from the study of single delay differential equations which show fundamental changes in the nature of solutions and novel effects that are absent in a non-delayed system (Ramana Reddy et al., 1998).

Time delay is found to introduce significant changes in the character and onset properties of the various collective regimes such as amplitude death and phase-locked states. Some results are novel and somewhat surprising – such as time delay induced death in an assembly of identical oscillators or the existence of clustered chimera states (Dodla et al., 2004; Sethia et al., 2008).

## Set Up of the MFA Method

The mean field approach (MFA) is developed and presented in our previous paper (Burić et al., 2010) and is based on a set of approximations that replace a many component system by a simpler system described by a small number of (averaged) collective or macroscopic properties. One should note that although the MFA has been applied to systems of excitable neurons with noise but with no time-delay (Zaks et al., 2005) and applied to large clusters of noisy neurons with time-delayed interaction by Hasegawa (2004), the approximations made in these papers resulted in a system of equations that is still too large to be analyzed analytically, so that the approximate system must be studied numerically. Results of our MFA approach is a simple system which allows analytical treatment of bifurcations and the parameter domains of stability of the stationary states which is in a quite good agreement with the exact complex system.

The MFA method is developed in the following way. Let us start from the system of excitable units whose dynamics is modelled by the set of stochastic delay differential equations (FitzHugh-Nagumo model):

$$\alpha dx_i = \left(x_i - \frac{x_i^3}{3} - y_i + I\right)dt + \frac{\beta}{N}\sum_{j=1}^{N}\left(x_j(t-\tau) - x_i\right)dt \qquad (1)$$

$$dy_i = (x_i + a)dt + \sqrt{2D}dW_i$$

where a, I, β, D and α<<1 are parameters. Excitable behavior represented by (1) reveals in destabilization of equilibrium though the occurrence of Hopf bifurcation. Each of N units in (1) is coupled with each other unit and with itself. The terms $(2D)^{1/2}dW_i$ represent the stochastic increments of independent Winere process: $E(dW_i) = 0$ and $E(dW_i dW_j) = \delta_{i,j}dt$, where E()denotes the expectation over many realizations of the stochastic process.

Our aim is to develop the approximate dynamical equations for the following mean fields:

$$X(t) = \frac{1}{N}\sum_i^N x_i(t) \equiv \langle x_i(t)\rangle$$

$$Y(t) = \frac{1}{N}\sum_i^N y_i(t) \equiv \langle y_i(t)\rangle \qquad (2)$$

For this purpose, we assume the following:

a) $x_i$ and $y_i$ have Gaussian distribution, which is true for D <<1,

b) $\frac{1}{N}\sum_i^N x_i \approx E(x_i)$, where E($x_i$) is the expectation with respect to the distribution of $x_i(t)$.

Concerning the assumptions (a) and (b), system (1) could be represented as the system of five deterministic delay differential equations for the variable (2) and the second order cumulants.

Let us introduce the deviations from the mean field:

$$n_{x_i}(t) = \langle x(t)\rangle - x_i(t)$$

$$n_{y_i}(t) = \langle y(t)\rangle - y_i(t) \tag{3}$$

where the average over the N units of the local variable xi is always denoted by bracket $\langle x\rangle$.

Furthermore, one could introduce the following correlations between centered moments:

$$s_x(t) = \langle n_x^2\rangle, s_y(t) = \langle n_y^2\rangle, u(t) = \langle n_x n_y\rangle \tag{4}$$

Based on the cumulant formulas:

$$\langle\langle x^2 y\rangle\rangle = 0 \rightarrow \langle x_i^2 y_i\rangle = Ys_x + YX^2 + 2Xu$$

$$\langle\langle x^3 y\rangle\rangle = 0 \rightarrow \langle x_i^3 y_i\rangle = 3s_x u + 3X^2 u + YX^3 + 3XYs_x$$

$$\langle x_i^2\rangle = s_x + X^2$$

$$\langle x_i^3\rangle = 3Xs_x + X^3$$

$$\langle x_i^4\rangle = 6X^2 s_x + X^4 + 3s_x^2$$
$$\langle x_i y_i\rangle = U + XY \tag{5}$$

Based on (3)-(5), using the Ito chain rule and by taking the average of the equations in (1), the following five deterministic delay differential equations are obtained:

$$\alpha\frac{dX}{dt} = X(t) - \frac{X(t)^3}{3} - s_x(t)X(t) - Y(t) + \beta(X(t-\tau) - X(t))$$

$$\frac{dY}{dt} = X(t) + a$$

$$\frac{\alpha}{2}\frac{ds_x(t)}{dt} = s_x(t)(1 - X(t)^2 - s_x(t) - a) - u(t)$$

$$\frac{1}{2}\frac{ds_y(t)}{dt} = u(t) + D$$

$$\frac{du(t)}{dt} = \frac{u(t)}{\alpha}(1 - X(t)^2 - s_x(t) - a) - \frac{1}{\alpha}s_y(t) + s_x(t) \qquad (6)$$

For the sake of further simplification, one can assume that the last three equations of (6) are equal to zero, if we consider that the relaxation time-scale of the first order moments is much slower then those of the second order moments. In that case, there is only one stationary state:

$$X(t) \equiv X_0 = -a$$

$$Y(t) \equiv Y_0 = \frac{-a}{2}\left[1 + \frac{a^2}{3} + a - (4D + (c + b^2 - 1)^2)^{1/2}\right] \qquad (7)$$

Analysis of the system (6) indicates the occurrence of the Hopf supercritical or subcritical bifurcations, as illustrated by bifurcation curves $\tau^j_{c,\pm}(\alpha)$ for fixed D, $a$ = 1.05 and $\tau^j_{c,\pm}(D)$ for fixed α, β = 1.05 (Figure 1).

Considering solutionsof the approximate system (6), these are checked against the solutions of the exact starting system (1), as it is shown in Figure 2. Results obtained indicate the following. When bifurcation diagrams of the approximate system (6) indicate stable solutions (states b,d,f and h in Figure 1), small stochastic fluctuations around the stationary state are observed in the exact system. On the other hand, when solutions of the approximate system (6) are unstable (states a,c,e and g in Figure 1), one finds stochastically stable periodic solution of the exact system (1). One should note that such agreement between the solutions of the exact (1) and approximate

(6) system stands only for small values of D, when local random variables have a Gaussian distribution. There is also a restriction on the values of interaction strength α, which should also be small, so the mean field approximation is valid for finite N. These restriction on the values of D and α indicate the developed MFA approach provides valid results only in cases when observed system is near the bifurcation curve. On the other hand, it could be easily shown there are no restrictions regarding the values of time delay.

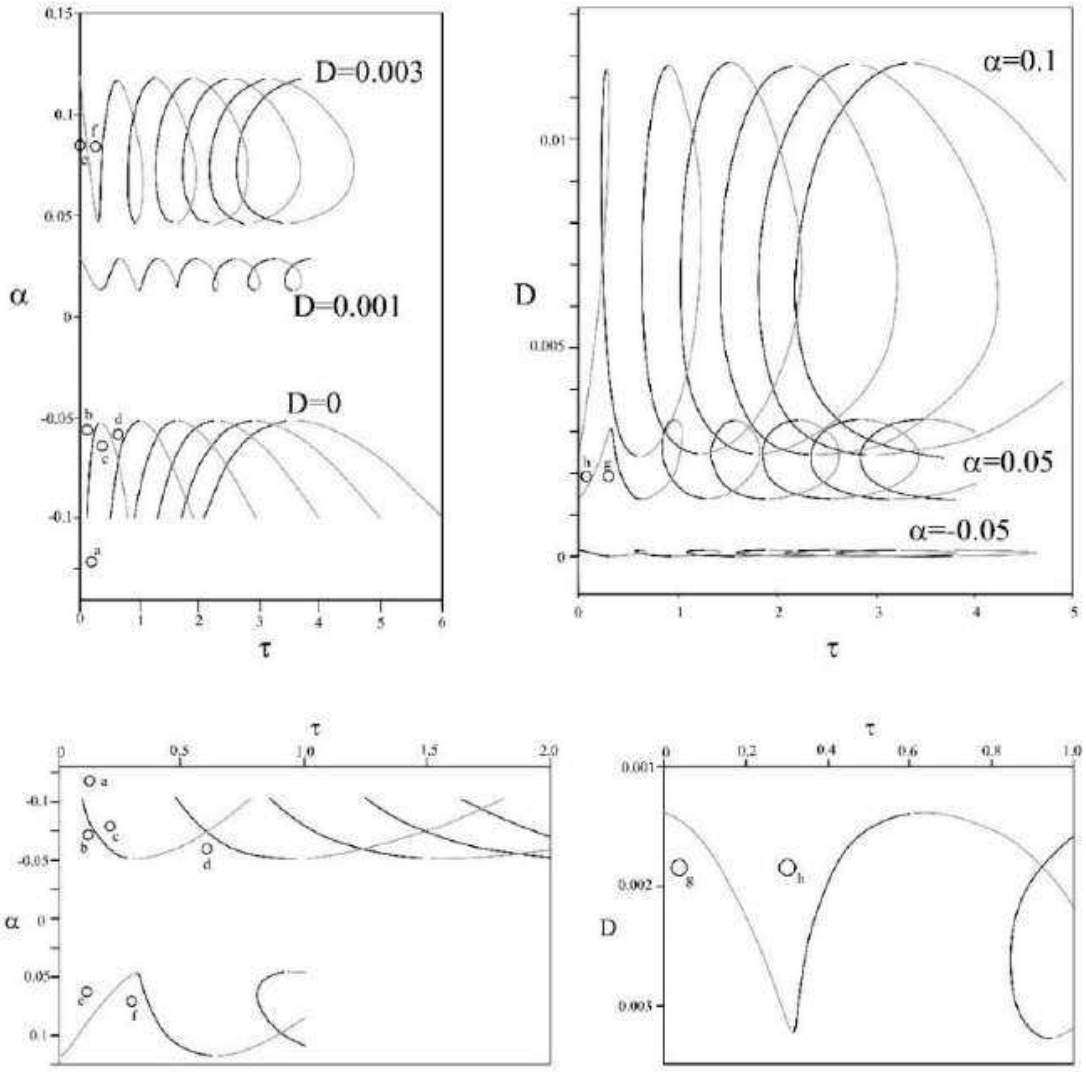


**Figure 1.** Bifurcation curves $\tau_{c,\pm}^{j}(\alpha)$ for fixed D, $a$=1.05 and $\tau_{c,\pm}^{j}(D)$ for fixed α, β = 1.05; β = 1.05. Gray curves correspond to $\tau_{c,-}^{j}$ and blac curves to $\tau_{c,+}^{j}$ for j = 0,1,2,3,4,5. Enlarged figures are shown in the lower part.

## Testing the Validity of MFA

We can further show the cases where both (a) and (b) hold, and scenarios where both (a) and (b) fail (separately showing that (a) and (b) are violated). In particular, both (a) and (b) hold if the local and global dynamics are characterized by a single attractor of the same type (fixed point or limit cycle) under the conditions the noise amplitude is small. Howvwe, if local and global dynamics are qualitatively different, or system under study exhibits multistability, (a) and (b) do not hold.

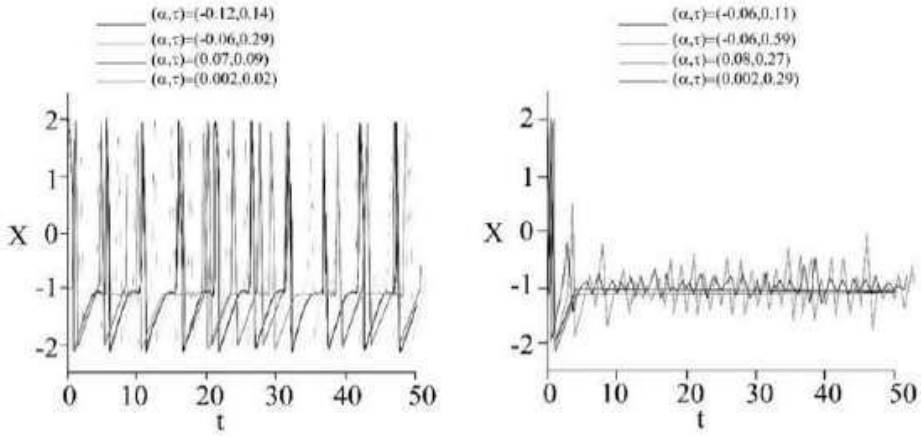


**Figure 2.** Time series of X(t) for the exact system (1) with 95 units.

As shown in Franović et al., (2014) (a) holds is the expectations qualitatively preserve the relaxation character of oscillations exhibited by the realizations. Franović et al., (2014) showed that the ratio of points lying on the transients compared to those lying on the slow branchens is small (0.1) over the sufficiently long time period along the trajectory ($E(x_{i,r}(t))$, $E(y_{i,r}(t))$. However, in case one assumes comparably larger noise amplitude, than noise-induced fluctuations are so large that the expectation varies from each of the realiyations at any t. Furthermore, we can estimate the rate at which the validity of (a) reduces with increasing noise level for fixed $\alpha$ and $\tau$. In order to do this, one needs to determine the maximal number of iteration steps $T_{max}$ for which the observed point in all the realiyations lies on the refractory branch. Figure 3 shows the fraction of realizations $N_{out}/N_r$ (for $T \leq T_{max}$, which represnts the number of steps for which the observed point has escaped the refractory branch) increasing with the noise level. In other words, Figure 3 clearly showsd the gradual loss of the validity of the assumption (a).

Regarding the conditions for the fulfillment of assumption (b), one may show these using indirect approach, derived from the corollary of the

formulation of the assumption itself. In particular, starting from the central limit theorem, by which the collective variables are normally distributed if the local variables are normally distibuted for finite N, the validity of the first assumption (a) for X(t) and Y(t) should imply that the local variables are independent. From normality tests on X(t) and Y (t) shown in Figure 4, one can see the validitiy of the assumption (a) for X(t) and Y(t), which also suggestes that the assumption (b) is valid. One should note that Figure 4 (c) indicates that distribution of $X_r(t_0+\delta t)$ follows Gaussian distribution, while $Y_r(t_0+\delta t)$ deviates from the Gaussian form, which is found for intermediate D and $\tau$.

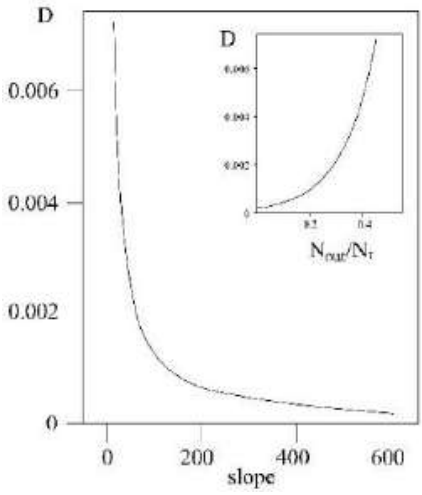


**Figure 3.** Slope of the curve of fraction of stochastic realizations $N_{out}/N_r$ ras a function of noise level D for $(\alpha,\tau)=(0.1,2.7)$. Inset denotes the actual change of $N_{out}/N_r$ with D.

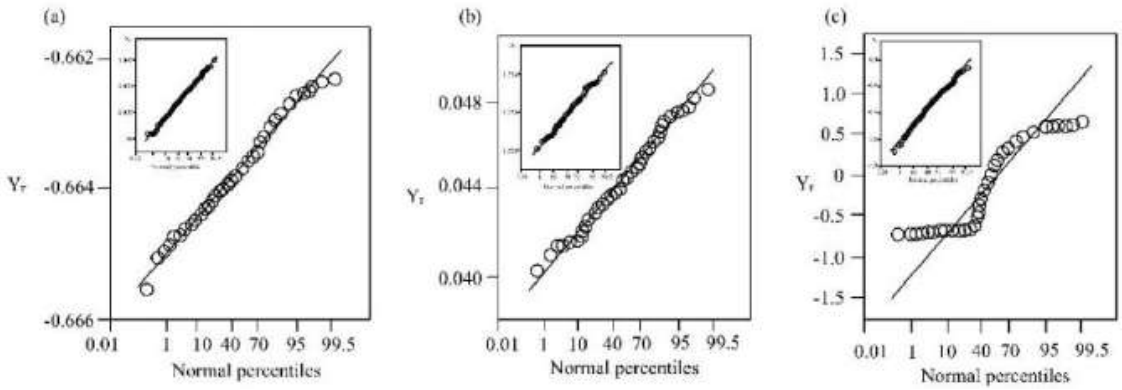


**Figure 4.** Graphic normality tests fort he collective variables X(t), Y(t). The parameter sets are: $(\alpha, D, \tau) = (0.1, 0.0002, 0.2)$ in (a), $(\alpha, D, \tau) = (0.1, 0.0002, 2.7)$ in (b), $(\alpha, D, \tau) = (0.1, 0.003, 1.5)$ in (c).

Apart from previous, one could also show that the occurrence of noise-induced bistability in dynamics of (6), provides the conditions for the failure of the assumption (b). In particular, due to global bifurcations, mean-field model (6) exhibits two types of bistable regimes: the coexistence of equilibrium state and periodic motion, and the coexistence of two limit cycles. Parameter values indicating bistability between the fixed point and limit cycle are indicated in Figure 5(a) by triangles, for which the inverse subcritical Hopf bifurcation stabilizes the equilibrium. In these two instaces, the assumption (b) is violated. As an illustration, phase portraits corresponding to the two attractors of the mean-field model and the appopriate orbits (which are not normally distributed around the respective averages) for the collective variables of the starting original system are given in Figure 5(b). Similar explanation stands for the coexistence of two limit cycles, where incipient cycle from the direct supercritical Hopf bifurcation coexist with the large cycle from the global biffurcation (indicated by the squares). It could be shown that assumption (b) is not valid in both of these instances.

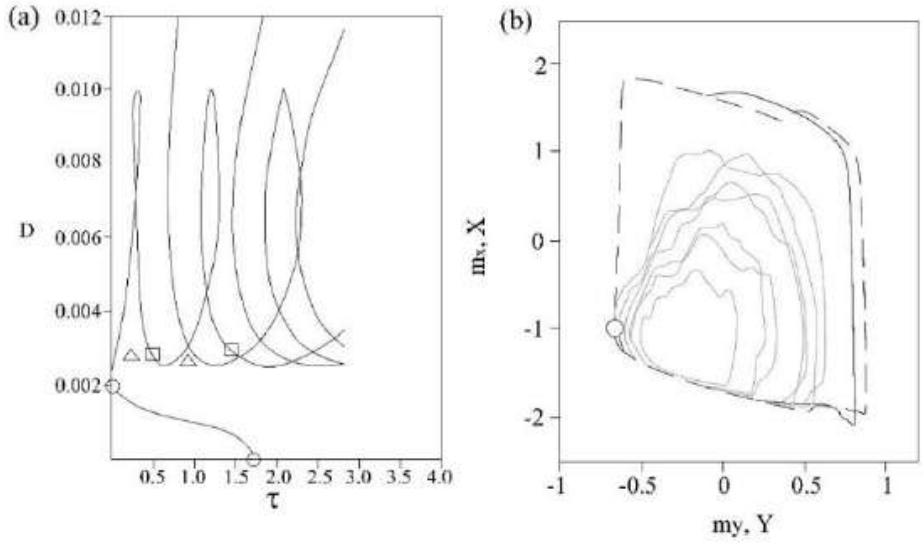


**Figure 5.** (a) Hopf bifurcation curves $\tau_{\pm}^{j}(D)$ fort he mean-field model. Triangles and squares indicate the parameter set for which the bistable dynamical regime exists. Black lines indicate the position of the direct (supercritical) Hopf bifurcation, while gray lines denote the position of inverse (subcritical) Hopf bifurcation. Curves are obtained for α=0.1; (b) Phase portrait $m_y, Y$-$m_x, X$ indicating bistability in the approxiate model: dot indicates fixed point, black dashed line indicates limit cycle from the global fold-cycle bifurcation, dark gray soild line ist he typical orbit (X(t), Y(t)) of the exact system, which fluctuates between the two attractors od the mean-field model. The parameter set is: (α, D, τ) = (0.1, 0.0029, 0.3).

## Role of Random Noise in Earthquake Nucleation

One can confirm the presence of random noise in real seismic motion by analyzing the recordings of the real observed fault motion. As shown in our previous paper (Vasović et al., 2016), displacement data recorded at 20 different GPS stations uniformly distributed along the active segments of San Andreas transform fault belong to a class of random temporally uncorrelated series.

Illustration of the effect of random noise on the seismic fault motion we start by analyzing the dynamics of spring-block model with all-to-all coupled blocks:

$$\frac{dx_i(t)}{dt} = y_i(t)$$

$$\frac{dy_2(t)}{dt} = \left\{-x_i(t) + F(y_i + v) - F(v) + \frac{K}{N}\sum_{j=1}^{N}\left[x_j(t-\tau) - x_i(t)\right]\right\}dt + \sqrt{2D}dW_i \quad (8)$$

where $x_i$ and $y_i$ represent displacement and velocity of the i-th block, $K$ is the spring constant (equal for all blocks), $F$ is the friction force, $F(V) = -(\mu_0 + b\,ln(V))$, $\mu_0$ is a steady-state friction, $b$ represents a material property which depends on different temperature and pressure conditions, $\tau$ is time delay (equal for all blocks) and $v$ is a nondimensional pulling background velocity. Terms $\sqrt{2D}dW_i$ represent stochastic increments of independent Wiener process, i.e., $dW_i$ satisfy:$E(dW_i) = 0, E\left(dW_i dW_j\right) = \delta_{ij}dt$, where $E()$ denotes the expectation over many realizations of the stochastic process and $D$ is intensity of additive local noise.

All to all coupling of units could be explained by the long-range itneractions observed in real conditions in the Earth's crust. In particular, according to Sanders (1993) San Jacinto fault zone affect the Mojave segment of San Andreas fault, since both exhibit similar seismic cycle of about 150 years. Motivation for interoduction of time delay comes from n the original work of Burridge and Knopoff (1967), who showed that there is a delayed interaction among cluster of blocks, with the intensity of time delay determined by the viscous properties along the specified fault segment.

By applying MFA approach, one could derive the following mean-field model:

$$\dot{m}_x(t) = m_y(t),$$
$$\dot{m}_y(t) = -m_x(t) + b\,ln\,v - b\,ln(m_y + v) + \frac{b}{2}\frac{1}{(m_y+v)^2}s_y + \frac{b}{4}\frac{1}{(m_y+v)^4}3s_{U_y}^2 +$$
$$+K\left[m_{U_x}(t-\tau) - m_{U_x}(t)\right]$$
$$\frac{1}{2}\dot{s}_{U_x}(t) = s_{U_xU_y}$$
$$\frac{1}{2}\dot{s}_{U_y}(t) = s_{U_y}\left[-\frac{a}{(m_{U_y}+v)} - \frac{a}{(m_{U_y}+v)^3}s_{U_y}\right] - (K+1)s_{U_xU_y} + D$$
$$\dot{s}_{U_xU_y} = -s_{U_xU_y}\left[\frac{a}{(m_{U_y}+v)} + \frac{a}{(m_{U_y}+v)^3}s_{U_y}\right] - (K+1)s_{U_x} + s_{U_y}(t) \quad (9)$$

where

$m_{U_x}(t) = \langle U_x(t)\rangle$, $m_{U_y}(t) = \langle U_y(t)\rangle$, $s_{U_x}(t) = \langle n_{U_x}^2(t)\rangle$, $s_{U_y}(t) = \langle n_{U_y}^2(t)\rangle$, $s_{U_xU_y}(t) = \langle n_{U_y}\cdot n_{U_x}\rangle$ and $n_{U_j}(t) = m_{U_j}(t) - U_{ji}(t), j = 1,2.$

Numerical analysis of system (9) indicates the occurrence of transition from equilibrium state to periodic oscillations for certain parameter values, Figure 6. As in Vasović et al., (2016) it could be shown that MFA model (9) exhibits qualitatively same dynamics before after the transition over the bifurcation curve as the starting stochastic model.

Further analyis of MFA model indicates the possible existence of bistability, depending on the initial conditions. In particular, if the initial conditions are set near the fixed point, then MFA model is in equilibrium, regardless of parameter values. Nevertheless, if initial conditions are set away from the fixed point, MFA model could exhiti erither equilibrium state of periodic motion depending on the parameter values "under" the bifurcation curve. One could claim that this bi-stable regime actually represents the seismogenic fault motion. This could be corroborated by the analysis of event magnitude distribution in the observed spring-block model, where magnitude of an event is defined as a natural logarithm of displacement sums for all blocks, while an event is defined as a peak (local maximum) of mean

displacement of starting system above a certain threshold (M = 0, average ratio of velocity sums to the introduced noise is at least $10^2$). Results of such analysis indicate that Gutenberg-Richter power law is followed by the recorded event magnitudes, with the b-value in the range (0.90-1.06), which corresponds well to the real observed data, Figure 7.

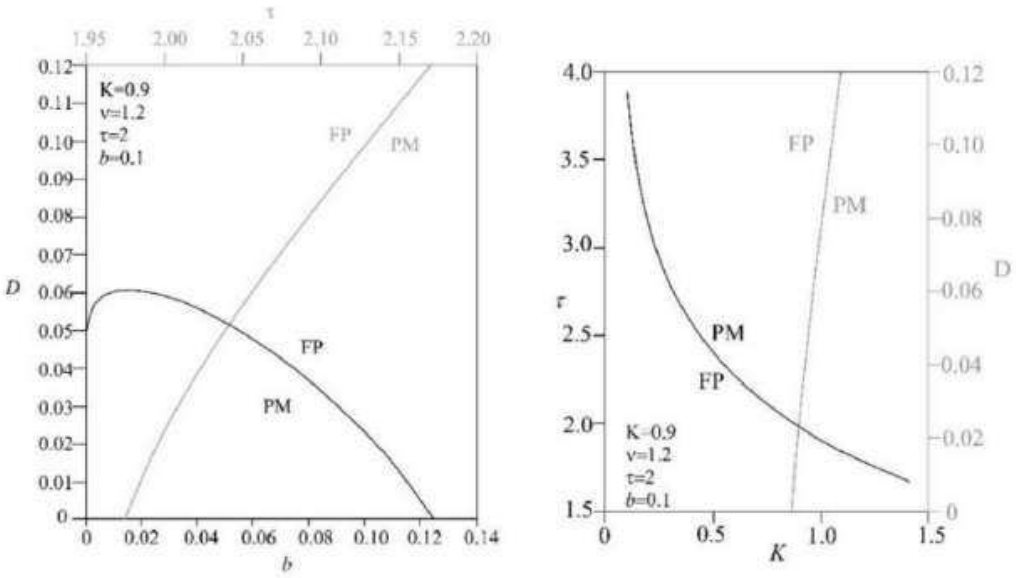


**Figure 6.** Bifurcation diagrams *a-D, K-D*, *K-τ* and *τ-D* for MFA model (9). FP denotes the region of fixed point (equilibrium state), while PM denotes the regime of periodic motion (regular periodic oscillations).

Effect of noise on the movement along the seismogenic fault is could also be illustrated by through dynamics of Burridge-Knopoff spring-slider model with the appropriate friction law (Kostić et al., 2017), whereby each block *i* interacts only with 2K nearest neighbors (instead of all-to-all coupling), including the effect of random noise:

$$\frac{dx_i}{dt} = y_i$$

$$\frac{dy_i}{dt} = -x_i + F(y_i + y_0) - F(y_0) + \frac{\alpha}{N}\sum_{j\in J}\left(x_{i+j}(t-\tau) - x_i\right) + \sqrt{2D}\xi_i(t), \qquad (10)$$

where

$x$ – block displacement,

$y$ – block velocity,

$\alpha$ - coupling strength in an one-dimensional array of blocks where a given block is coupled to K of its neighbors on each side; blocks at the end of the array are connected to neighboring blocks only on one side,

$\tau$ – uniform time delay of the order of the adopted viscous time constant in the original Burridge-Knopoff model,

$y_0$ - pulling velocity of the upper moving plate,

$\xi_i(t)$ - independent Gaussian white noise terms, such that $\langle \xi_i \rangle = 0, \langle \xi_i \xi_j \rangle = \delta_{ij}$ holds,

$J$ - set of indices $J = \{-K, ..., K\} \setminus \{0\}$,

$F$ - rate-dependent friction law: $F(y) = \mu_0 - b\, ln(y)$, where $\mu_0$ is a steady-state friction, and $b$ represents a material property which depends on the temperature and pressure conditions.

As addition to the previous analysis of dynamics of a model with globally coupled units, we also investigate the effect of the range of interactions on the fault dynamics, from the nearest-neighbor interactions up to a globally connected assembly of blocks.

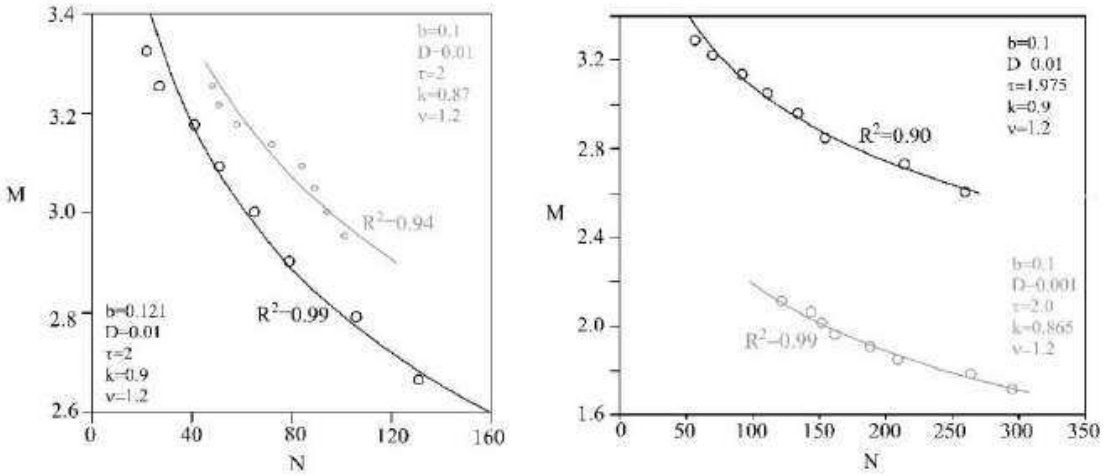


**Figure 7.** Magnitude-frequency distribution for different parameter values follows the Gutenberg-Richter law with satisfying statistical accuracy, while the corresponding b-value is in the range of real observed data.

By applying the aforementioned MFA method, one could derive the mean-field model for collective dynamics of $N$ blocks with $2K$ nearest-neighbor interactions:

$$\frac{dm_x}{dt} = m_y$$

$$\frac{dm_y}{dt} = -m_x - F(y_0) + F(y_v + y) + \frac{1}{2}F''(m_y + y_0)S_y + \frac{2K\alpha}{N}(m_x(t-\tau) - m_x)$$

$$\dot{S_x} = 2X$$

$$\dot{S_y} = -2X\left(1 + \frac{2K\alpha}{N}\right) + 2F'(m_y + y_0)S_y + 2D$$

$$\dot{X} = S_y - S_x\left(1 + \frac{2K\alpha}{N}\right) + F'(m_y + y_0)X \qquad (11)$$

where $X = \frac{1}{N}\sum_{i=1}^{N} x_i$ and $Y = \frac{1}{N}\sum_{i=1}^{N} y_i$ are the macroscopic variables, $m_u = \langle u_i \rangle = \frac{1}{N}\sum_i u_i$ and $m_v = \langle v_i \rangle = \sum_i v_i$ are the means, $s_u = \langle \delta u_i^2 \rangle = \langle (u_i - m_u)^2 \rangle = \langle u_i^2 \rangle - {m_u}^2$ and $s_v = \langle \delta v_i^2 \rangle = \langle (v_i - m_v)^2 \rangle = \langle v_i^2 \rangle - {m_v}^2$ are the associated variances and the covariance is $U = \langle \delta u_i \delta v_i \rangle = \langle (u_i - m_u)(v_i - m_v) \rangle = \langle u_i v_i \rangle - m_u m_v$. Detailes of the derivation of (2) could be found in Kostić et al., (2017).

System (11) could be further simplified by taking into account only the mean values of displacement and velocity, which is justified considering very small deviations from the mean displacement and velocity:

$$\frac{dm_x}{dt}(t) = m_y(t)$$

$$\frac{dm_y}{dt}(t) = -m_x(t) + b\,ln(y_0) - b\,ln(m_y + y_0) + \frac{1}{2}\frac{D}{(m_y + y_0)} + \frac{2K\alpha}{N}\left(m_x(t-\tau) - m_x(t)\right) \qquad (12)$$

Mean-field model (12) has a unique stable stationary solution ($m_x$, $m_y$) = $(\frac{D}{2y_0}, 0)$. Condition for the existence of a nontrivial solution is given by the characteristic equation:

$$\lambda^2 + \frac{\lambda}{y_0}(a + \frac{D}{2vy_0}) + 1 + \frac{2K\alpha}{N}(1 - e^{-\lambda\tau}) = 0. \qquad (13)$$

After some algebra, the expression for the critical coupling delay is given in the following form:

$$\tau = \frac{1}{\omega} arctg \frac{\frac{\omega}{y_0}(b + \frac{D}{2y_0})}{\omega^2 - (1 + \frac{2K\alpha}{N})} \qquad (14)$$

It could be shown that MFA model (10) undergoes Andronov-Hopf bifurcation, illustrated by multiple branches of Hopf bifurcation curves given by $\tau_{\pm j}\pi$, where $j = 0,1,2,\ldots$. In present case, only on the first bifurcation curve is in the focus. As one can see from Figure 8, there is a supercritical Andronov-Hopf bifurcation from equilibrium state to periodic motion, triggered by increasing time delay in interaction among the coupled blocks. For time delay $\tau < 0.9$ there is no bifurcation, indicating that the impact of delayed interaction is crucial for the occurrence of instability. However, bifurcation may also occur for a constant τ solely by increasing the number of interacting blocks. This means that in the case when different fault segments along the seimogenic fault are in delayed interaction, seismic fault motion could be induced solely by increasing the active displacement length. One should note that in case block is coupled only to its nearest neighbors, time delay does not induce the instability.

Validity of MFA approach is proved by the qualitatively the same dynamics for the starting exact system and the MFA model (12), as it is done in Kostić et al (2017). Moreover, one could show that oscillation frequencies of the starting and the approximate system above the bifurcation curve are almost identical, while the difference in respective amplitudes of periodic motion is acceptable.

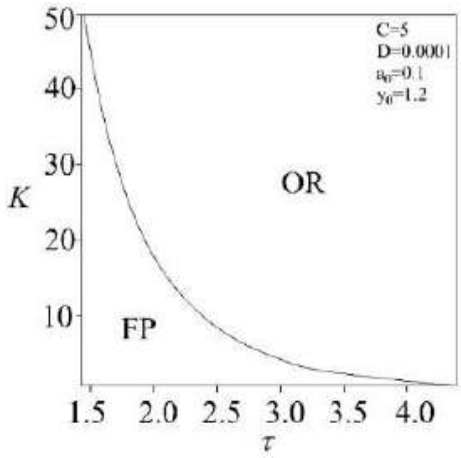


**Figure 8.** *K(τ)* bifurcation curve describing the destabilization of equilibrium in the MFA model (10) via Andronov-Hopf bifurcation. FP and OR denote the fixed point and periodic oscillations, respectively.

If one examines the effect of noise on the fault displacement, it could be concluded that this effect is not significant for the expected ratio of coseismic slip rate vs. seismic noise is in the range $10^{-2}$-$10^{-7}$, i.e., there are no significant changes in dynamics of MFA system for seismic noise up to 0.1. However,

for small $K$ and higher values of seismic noise, increase of time delay does not give rise to bifurcation, i.e., noise suppresses the onset of instability in the observed system. As for the effect of coupling strength α, increase of α leads to occurrence of bifurcation under the condition of delayed interaction among the blocks in the observed system (black lines in Figure 9). Further inquiries show that for small α there is a boundary value of $K$ below which the effect of time delay is insignificant. Regarding the impact of friction, it seems that decrease of friction leads to the occurrence of inverse supercritical Andronov-Hopf bifurcation (gray lines in Figure 9). From the seismological viewpoint, this finding could indicate that for the fault which is in stationary aseismic motion, in case a reduction of friction occurs (due to effect of pore water or similar), one could expect onset of seismic motion, under the condition that delayed interaction exists between different fault segments.

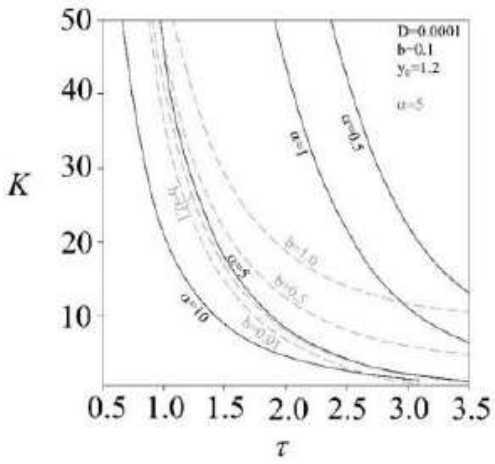


**Figure 9**. Bifrcation curves for the MFA model for different values of coupling strength (α) and friction parameter (b).

Regarding the similarity of the movement of theblocksin the starting system and the real displacements along the fault, we could consider that magnitude of a single event M is a natural logarithm of a sum of squares of displacements for coupled blocks with the largest displacements in the observed array $x_i$:$M = ln\left(\sum_{i=1}^{N}(x_i)^2\right)$, where $N$ is the total number of blocks in the starting system. One can clearly see the irregulardistribution of magnitude over time, which qualitatively resembles the real observed magnitude distribution, Figure 10.

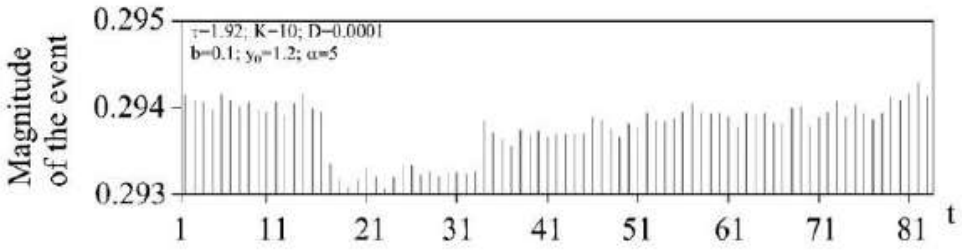


**Figure 10.** Temporal distribution of displacement sums for a group of blocks with largest displacements in the starting exact system.

## Role of Colored Noise in Earthquake Nucleation

Apart from the real observed random noise, as shown by investigating displacement along the active parts of San Andreas fault (Vasović et al., 2016), one can also find traces of colored noise in situ. For instance, in our previous paper (Kostić et al., 2020) we examined strike-slip fault movement directly measured at the two points in Driny cave, Male´ Karpaty mts in Slovakia (Brienstensky et al., 2011), Figure 11, and ambiental noise measurements before and after the earthquake on 8th September 2015 at the BKS station (Byerly Seismogrpahic Vault, Berkley). For strike-slip movement in Driny cave, we show that error of the established prediction model is autocorrelated, while the background seismic noise before and after the earthquake recorded at BKS station is showed to exhibit properties of colored noise.

Results of the analysis of the real fault displacement in Driny Cave indicate the these movement could be sufficiently accurately described by the Fourier series sums of sine and cosine functions in the following general form:

$$y = a_0 + a_1 \cdot cos(\omega \cdot t) + b_1 \cdot sin(\omega \cdot t) + a_2 \cdot cos(2 \cdot \omega \cdot t) + b_2 \cdot sin(2 \cdot \omega \cdot t) + \ldots, \quad (15)$$

where $a_i$ and $b_i$ are Fourier coefficients, and $\omega$ is the average oscillation freuqency. Coefficients and frequencies of the resulting models for estimation of displacements at the locations Driny 1 and Driny 3 are given in our previously published paper (Kostić et al., 2020).

Using the suggested estimation expression (13) and the corresponding coefficient values (Table 1 in Kostić et al., 2020), one could establish satisfying prediction accuracy (Figure 12).

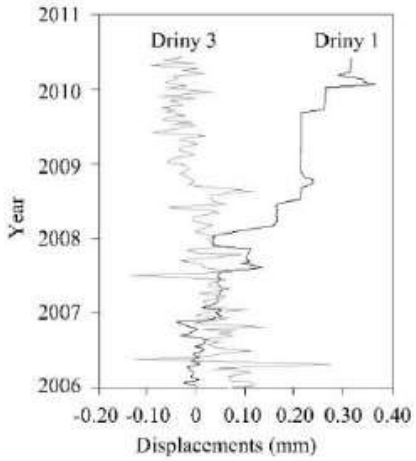


**Figure 11.** Analyzed strike-slip displacements along the faults at Driny Cave (Brienstensky et al., 2011).

For both the fault displcements in Driny cave, results of Durbin-Watson statistics indicate the presence of autoccorelation in the recorded noise, while for the recorded noise before and after the earthquake on 8th September 2015 at the BKS station autocorrelation function indicates the presence of autocorrelation.

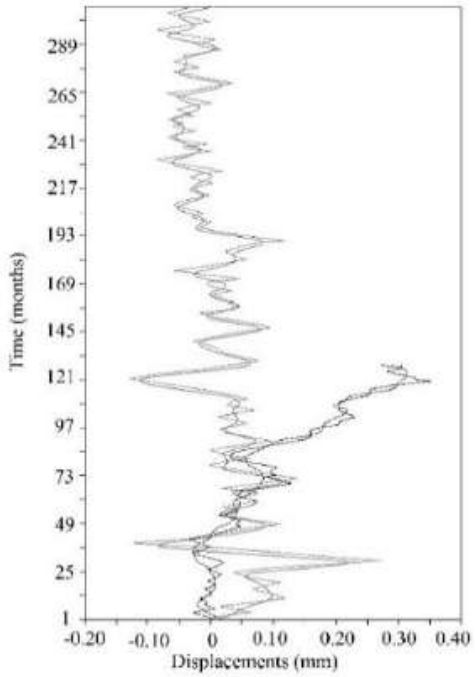


**Figure 12.** Real observed fault displacement (continuous line) vs the estimated motion (dashed line). Estimation accuracy for Driny 1 (left), black lines: R2 = 0.97, MSE = 0.00017, for Driny 3 (right), gray lines: R2 = 0.85, MSE = 0.0005.

Conducted analysis of the real observed fault displacements and background seismic noise confirmed the presence of colored noise in the real conditions, so the introduction of the correlated noise in the existing dynamical models of earthquake nucleation is justified. Similarly to the previous case with random noise, dynamics of seismogenic fault motion is described by the spring-block model ofall-to-all coupled blocks:

$$\dot{u}_i(t) = v_i(t)$$

$$\dot{v}(t) = -u_i(t) + F(v_i + v) - F(v) + \frac{K}{N}\Big(u_j(t-\tau) - u_i(t)\Big) + Z_i(t)$$

$$dZ_i(t) = -\frac{Z_i}{\varepsilon}dt + \sqrt{\frac{2D}{\varepsilon}}dW_i \qquad (16)$$

where $u_i$ and $v_i$ are displacement and velocity of the $i$-th block, $K$ is the spring constant, $F$ is the friction force $F(V) = -(\mu_0 + b\,ln(V))$, $\tau$ is time delay and $v$ is nondimensional pulling background velocity. $Z_i(t)$ is an Ornstein-Uhlenbeck process, terms $\sqrt{(2D/\varepsilon)}dWi$ represent stochastic increments of independent Wiener process, i.e., $dW_i$ satisfy: $E(dWi)=0$, $E(dW_i dW_j)=\delta_{ij}dt$, where $E(\,)$ denotes the expectation over many realizations of the stochastic process, $\varepsilon$ is the noise correlation time and $D$ is the intensity of noise.

By using MFA approach, and by introducing deviations from the mean-field:

$$\langle u(t)\rangle = \lim_{N\to\infty}\frac{1}{N}\sum_{i=1}^{N} u_i(t),$$

$$\langle v(t)\rangle = \lim_{N\to\infty}\frac{1}{N}\sum_{i=1}^{N} v_i(t),$$

$$\langle z(t)\rangle = \lim_{N\to\infty}\frac{1}{N}\sum_{i=1}^{N} z_i(t),$$

for each element $n_u(t) = \langle u(t)\rangle - u(t), n_v(t) = \langle v(t)\rangle - v_i(t), n_z(t) = \langle z(t)\rangle - z_i(t)$, where ee assume that these fluctuations are Gaussian and statistically independent in different elements, and by applying Ito's chain rule:

$$dX = Fdt + GdW$$

$$V(t) = U(u,t)$$

$$dV = \frac{\partial U}{\partial t}dt + \frac{\partial U}{\partial u}dX + \frac{1}{2}\frac{\partial^2 U}{\partial xu^2}G^2 dt$$

one can arrive at the following mean-field model:

$$\dot{m}_u = m_v$$

$$\dot{m}_v = -m_u - b\,ln(m_v + v) + b\,ln(v) + \frac{1}{2}\frac{b}{(m_v+v)^2}s_v + \frac{3}{4}\frac{b}{(m_v+v)^4}{s_v}^2 + K(m_u(t-\tau) - m_{xu}) + m_z$$

$$\dot{m}_z = -\frac{1}{\varepsilon}m_z$$

$$\frac{1}{2}\dot{s}_u = U_{uv}$$

$$\frac{1}{2}\dot{s}_v = s_v\left[-\frac{a}{m_v+v} - \frac{a}{(m_v+v)^3}s_v\right] - (K+1)U_{uv} + U_{vz}$$

$$\dot{U}_{uv} = U_{uv}\left[-\frac{a}{m_v+v} - \frac{a}{(m_v+v)^3}s_v\right] - (K+1)s_u + s_v + U_{uz}$$

$$\dot{U}_{uz} = U_{vz} - \frac{1}{\varepsilon}U_{uz}$$

$$\dot{U}_{vz} = -U_{uz} - \frac{a}{m_v+v}U_{vz} - \frac{a}{(m_v+v)^3}s_v U_{vz} - KU_{uz} + D - \frac{1}{\varepsilon}U_{vz} \qquad (17)$$

where

$m_x(t) = \langle x(t)\rangle, m_x(t-\tau) = \langle x(t-\tau)\rangle, m_y(t) = \langle y(t)\rangle, m_z(t) = \langle z(t)\rangle$ are the means, $s_x(t) = \langle n_x^2(t)\rangle, s_y(t) = \langle n_y^2(t)\rangle, s_z(t) = \langle n_z^2(t)\rangle$, are the mean square deviations, and $U_{xy}(t) = \langle n_x n_y\rangle, U_{xz}(t) = \langle n_x n_z\rangle, U_{yz}(t) = \langle n_y n_z\rangle$ are the cross-cummulants.

Numerical analysis of the model (15) indicates the occurrence of direct Andronov-Hopf bifurcation, from the steady stationary movement (denoted as

equilibrium state) to regular and irregular oscillations of small and high amplitude (respectively), Figure 13.

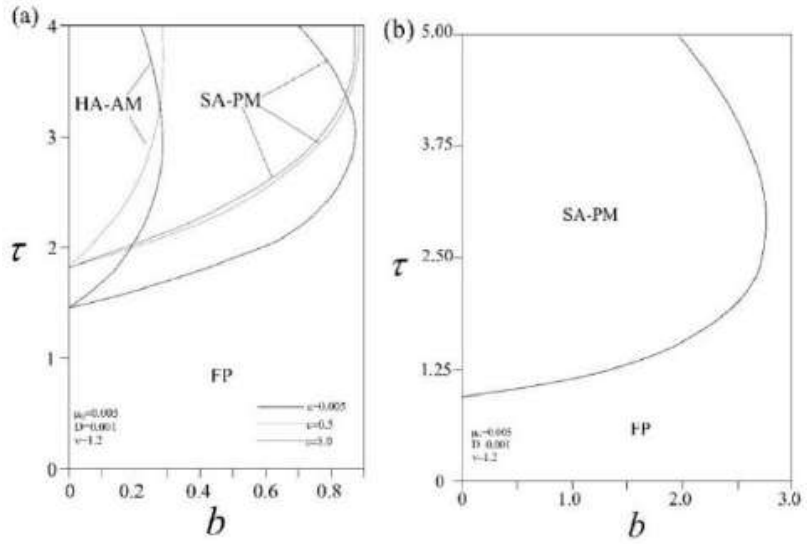


**Figure 13.** Bifurcation diagrams $b$-$\tau$ for different values of $\varepsilon$. FP denotes the steady stationary displacement (fixed point), SA-PM stands for the small-amplitude periodic motion, while HA-AM denotes the high-amplitude aperiodic motion, (a) K = 1, (b) K = 5.

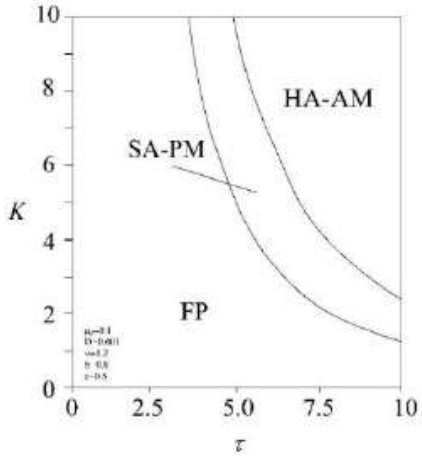


**Figure 14.** Bifurcation diagram K-$\tau$. FP denotes the steady stationary displacement (fixed point), SA-MP stands for the small-amplitude periodic motion, while HA-AM denotes the high-amplitude aperiodic motion.

One could see from Figure 13a, that here are no high-amplitude oscillations for high values of $\varepsilon$, which could indicate that degree of autocorrelation of background seismic noise directly determine the transition from equilibrium state either to low-amplitude oscillations or to high-amplitude aperiodic motion, considered as the onset of the seismogenic fault

motion. One could note that further increase of K further excludes the possibility of the occurrence of seismogenic fault motion: for higher values of $K$ transition from steady stationary state to creep regime is possible even for higher values of friction $a$. From the seismological viewpoint, it seems that no seismogenic fault motion occurs for higher values of coupling strength (Figure 13b).

For the increased values of time delay, one could observe the high-amplitude aperiodic motion, which indicates that seismogenic fault motion occurs for higher delay in interaction between the neighboring patches of fault. In particular, it seems that without the delay in interaction, or with the small values of delay, the fault patches are locked withput the delay in interaction or with samll values of time delay, which further prevents the onset of seismogenic fault motion (Figure 14).

## Role of Noise in Groundwater Level Dynamics

Although groundwater level dynamics has been analyzed using different approaches (Hong, 2017; Adamowski and Chan, 2011; Suryanarayana et al., 2014; Sreekanth et al., 2011; Sahoo and Madan, 2013; Fallah-Mehdipour et al., 2013), the role of noise has not been previously examined. Existence of noise in real observed groundwater level (GWL) oscillations is confirmed by analyzing GWL oscillations from four piezometric stations in Serbia: Leskovac (2007-2013), Negotin (2004-2013), Kruševac (2004-2013) and Bogatić (2004-2013).

Recorded GWL oscillations are firstly subjected to surrogate data testing (Perc et al., 2009), which includes testing of the three null hypotheses: (1) data are independent random numbers drawn from some fixed but unknown distribution, (2) recordings originate from a stationary linear stochastic process with Gaussian inputs, (3) recordings originate from a stationary Gaussian linear process that has been distorted by a monotonic, instantaneous, time-independent nonlinear function. According to the results of surrogate data testing, $\varepsilon_0<\varepsilon$ for all generated surrogates, except for the recordings at Kruševac station, where $\varepsilon_0$ is within $\varepsilon$ for the first and the second hypothesis (Figure 15), which implies the significant impact of stochastic component. As for the GWL recordedings at other stations, results obtained indicate the significant stochastic influence, concerning almost the same trend of the original time series and surrogates with increasing prediction time steps for the first and the third null hypothesis, while larger differences between the

original and surrogate time series are observed for GWL oscillations at Leskovac station.

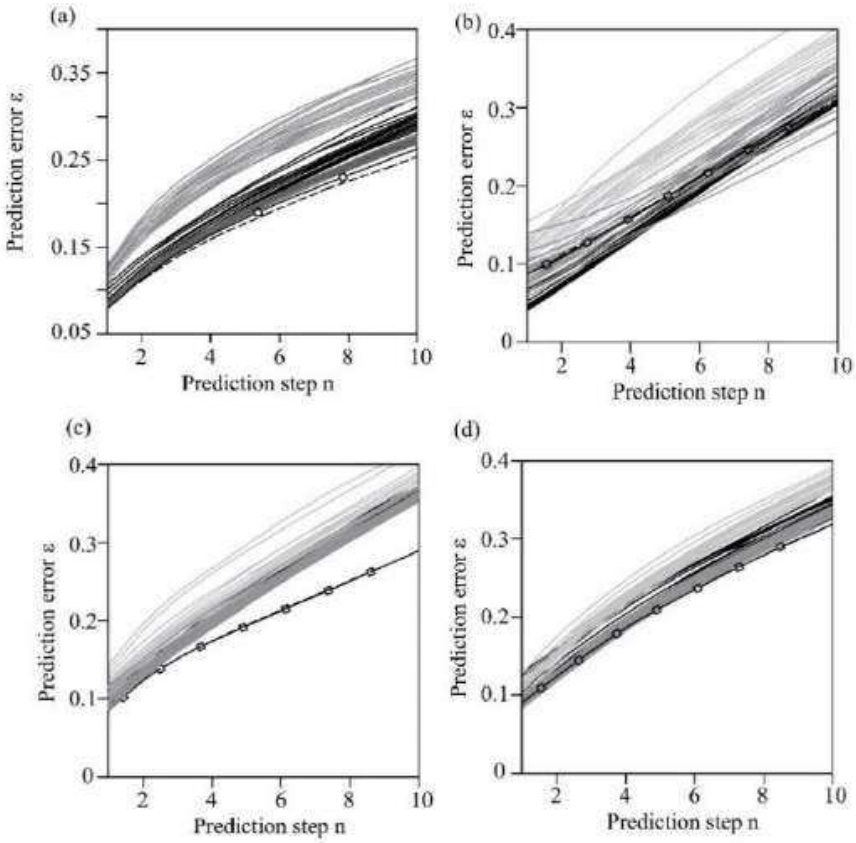


**Figure 15.** Surrogate data testing for GWL oscillations at the following stations: (a) Bogatić, (b) Kruševac, (c) Leskovac, (d) Negotin. Black line denotes evolution of $\varepsilon$ for the I null hypothesis, light gray for the II null hypothesis, dark gray for the III null hypothesis, while dashed line denotes the evolution of $\varepsilon_0$ for the I and the II null hypothesis, and fence line marks the evolution of $\varepsilon_0$ for the III hull hypothesis.

Significant influence of stochastic component in all the examined time series is further confirmed by the results of nonlinear time series analysis, i.e., determinism test, with low value of determinism coefficient, below 0.72, indicating strong presence of stochastic component.

If we apply the local-regression LOESS method (Loader, 1999), we can arrive at the conclusion that seasonal component of GWL dynamics could be represented as sum of finite sine and cosine harmonics of the general form:

$$Z_{SEASONAL}(t) = \sum_{i=1}^{N}(m_i \sin(2\pi f_i t) + n_i \cos(2\pi f_i t)) \; t = 1,\ldots,N, \tag{18}$$

where $m_i$ and $n_i$ are the Fourier coefficients $f_i$ is a frequency of seasonal harmonics and $N$ is a total number of significant harmonics. Residual components are obtained by subtracting $z_{seasonal}$ in Eq. (18) from observed daily water levels, and modelled with the ARMA model in the following manner (Box et al., 2008)

$$Z_{R,t} = \phi_1 Z_{R,t-1} + \phi_2 Z_{R,t-2} + \ldots + \phi_p Z_{R,t-p} + \varepsilon_t - \theta_1 a_{t-1} - \theta_2 a_{t-2} - \ldots - \theta_q a_{t-q} \quad (19)$$

where $Z_R$ is residual time series, $\varepsilon_t$ is the independent random series, $\phi_1$, $\phi_2$,..., $\phi_p$ are the parameters of the autoregressive model, and $\theta_1$, $\theta_2$,..., $\theta_q$ are the parameters of the moving-average model.

Results of modelling are shown in Figure 16, where recorded GWL oscillations are compared to the modelled seasonal component. One could see that trend of GWL osicllations is modelled with sufficient accuracy, while models fail to mimic peaks of the oscillations. This could be overcome by further modelling of residuals, or by introducing the stochastic component. In the latter case, one could propose the following dynamical system of GWL oscillations:

$$\frac{d(gwl)}{dt} = m \cdot sin(\omega t) + n \cdot cos(\omega t) - s \cdot g(t-\tau) - (gwl)^3 + z(t)\text{v}$$
$$dz(t) = -\frac{z}{\varepsilon} dt + \sqrt{\frac{2D}{\varepsilon}} dW \quad (20)$$

where $m$ and $n$ are Fourier coefficients, $s$ controls the effect of autocorrelation properties on the GWL dynamics. Variable $gwl$ stands for the groundwater level. Variable z(t) represents an Ornstein-Uhlenbeck process, and term $\sqrt{\frac{2D}{\varepsilon}} dW$ represents stochastic increment of independent Wiener process, i.e., dW satisfy: E(dW) = 0, where E() denotes the expectation over many realizations of the stochastic process.

Stochasticity in GWL oscillations could be further corroborated by Box-Jenkins approach, showing that the reduction of the number of harmonics gives rise to the impact of stochastic component (Figure 17).

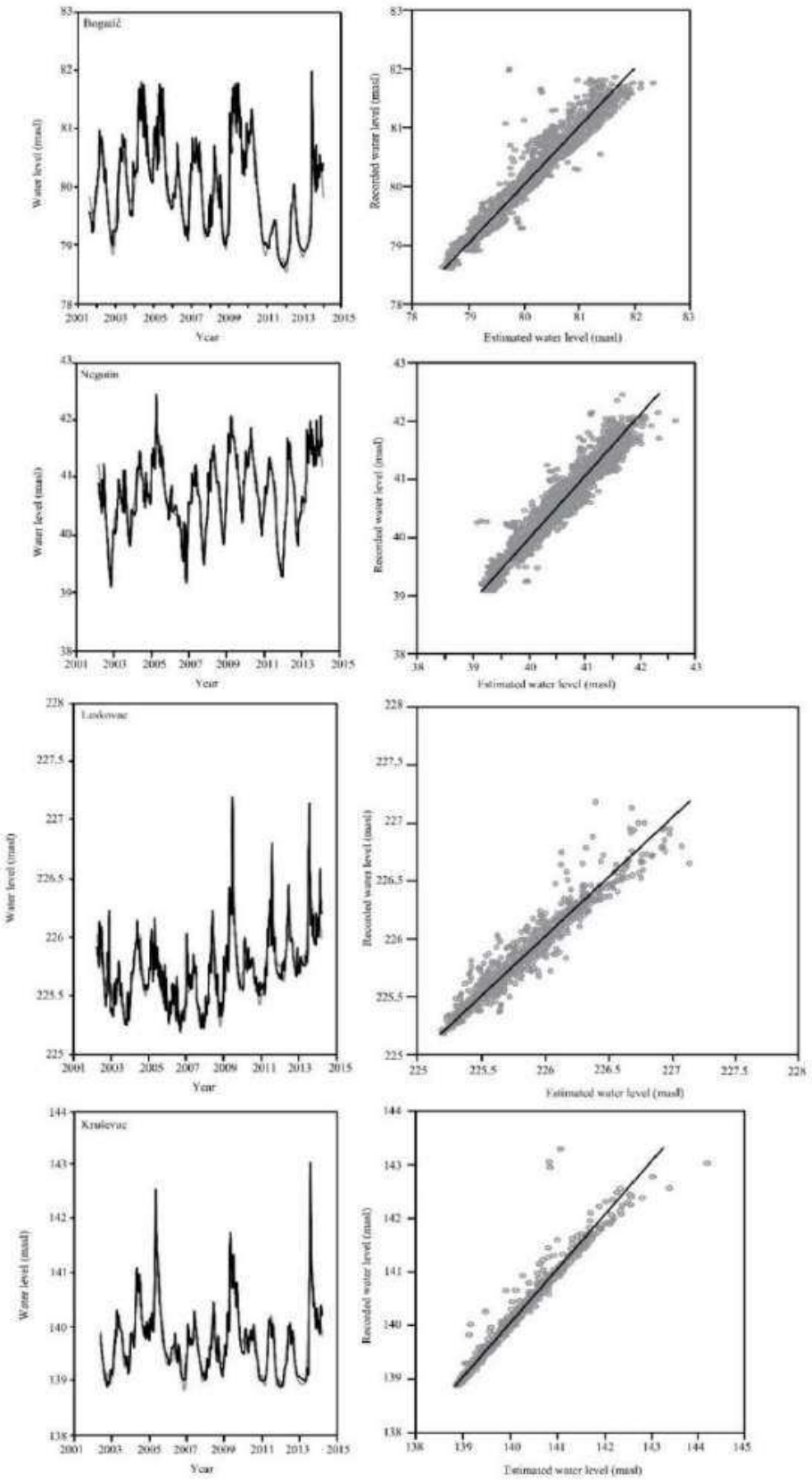


**Figure 16.** Observed GWL (black line) with the modelled seasonal component (gray line).

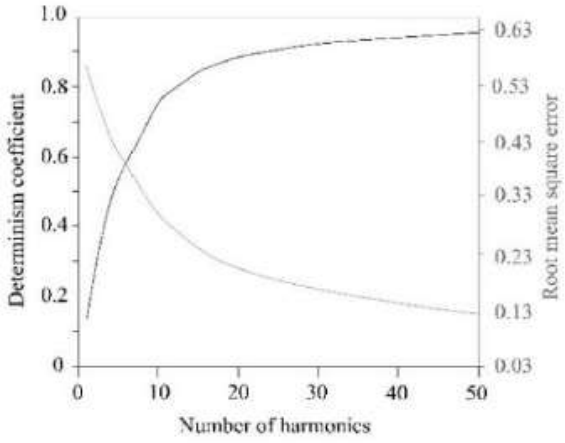


**Figure 17.** Reduction of the number of harmonics in GWL model leads to increase of the effect of stochasticity, for the recordeddata at Kruševac station.

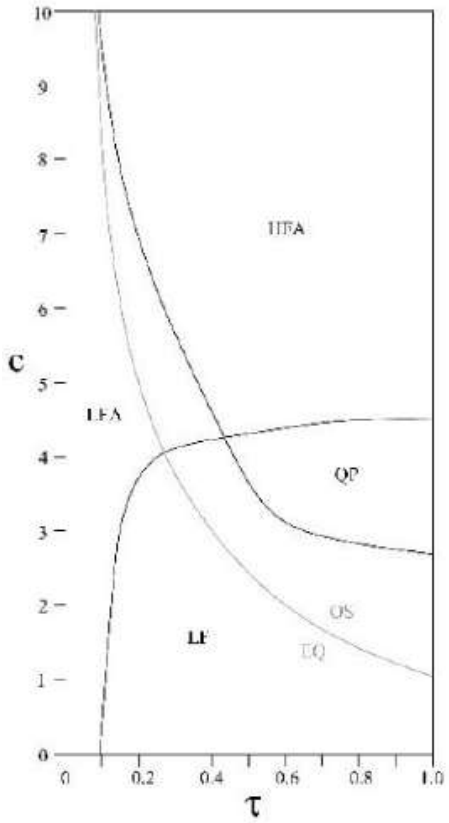


**Figure 18.** Bifurcation diagrams $\tau$-$c$: $\omega$=0 (gray line) and $\omega$=1 (black lines). Abbreviations are the following: EQ – equilibrium state, LF – low frequent oscillations, LFA – low frequent and amplitude oscillations, HFA - high frequent and amplitude oscillations, QP – quasiperiodic oscillations.

Results of standard numerical bifurcation analysis are shown in Figure 18. If there are no oscillations in the starting system ($\omega$ = 0), there is a transition from fixed point to steady stationary movement. However, if one

assumes oscillations in the starting deterministic system ($\omega$ = 1), there is a transition to different types of oscillation: from low frequent and moderate amplitude oscillations, over high frequent and high amplitude oscillations to quasiperiodic behavior. One should note that results of analysis indicate a gradual transition between different dynamical regimes: small-diameter cycle occurs first (after the fixed point becomes unstable), which is further followed by the increase in diameter, indicating possible direct supercritical Andronov-Hopf bifurcation.

It should be emphasized that if one takes into account the effect of noise, with the initial conditions are set away from the equilibrium state and the system near the bifurcation curve, one could obtain time series qualitatively similar to the recorded ones, as the one shown in Figure 19. Here we tooke the upper envelope of the obtained solution of system (20) using Hilbert transform:

$$gwl = F^{-1}\{G(f)\} + i\left[\frac{1}{\pi t}\cdot F^{-1}\{G(f)\}\right] \tag{21}$$

where G(f) is Fourier transform of the function g, i.e., solution of system (20), $F^{-1}$ is the inverse Fourier transform, and $i$ is the imaginary unit.

Possible further application of the suggested model (20) could be given in a model of landslide dynamics, initially suggested by Morales et al., (2017):

$$\frac{dx}{dt} = f * y$$

$$\frac{dy}{dt} = -\frac{k}{1+y} + G + h * g - x$$

$$\frac{d(gwl)}{dt} = m\sin\theta + n\cos\theta + z(t) - s\cdot g(t-\tau) - (gwl)^3 + z(t)$$

$$dz = -\frac{z}{\varepsilon}dt + \sqrt{\frac{2D}{\varepsilon}}dW$$

$$\frac{d\theta}{dt} = \omega \tag{22}$$

where $x$ corresponds to displacements, $y$ denotes the block velocity, $G$ is the gravity constant, $F$ is the velocity-dependent friction term. Parameters $k$, $f$ and $h$ represent the tuning parameters for tuning the effect of friction, displacement scales and influence of groundwater level oscillations, respectively.

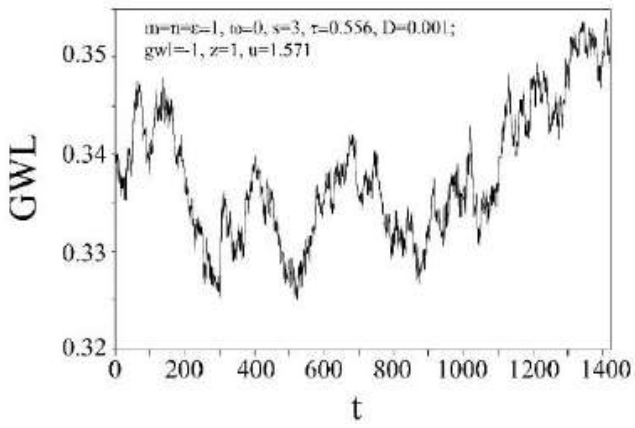


**Figure 19.** GWL time series as solution of the starting system (18) qualitatively similar to the recorded time series.

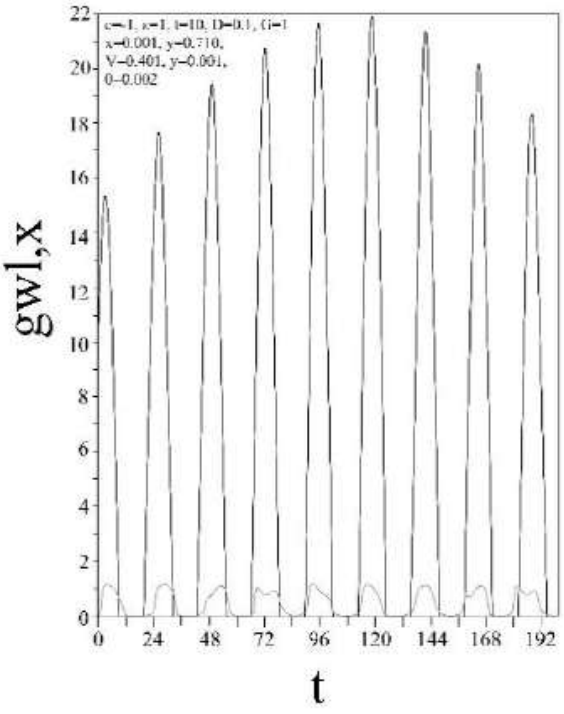


**Figure 20.** Movements along the slope (black line) and GWL oscillations (gray line).

Results of numerical analysis of system (22) indicate that GWL oscillations actually induce the block displacements (Figure 20), where

movements along the slope and GWL oscillations are obtained using the positive part of the solutions displacements and groundwatere level oscillations of the system (22): $nx^{+}, gwl^{+}(t) = max(x(t), gwl(t), 0) = \begin{cases} x(t), gwl(t), & if x(t), gwl(t) > 0 \\ 0, & otherwise \end{cases}$.

## Role of Noise in Excitable Systems

Excitability occurs in dynamical systems which are near transition between different dynamical régimes, e.g., from equilibrium state to periodic motion, where small perturbations induce the small-amplitude responses, while larger perturbations may lead to large-amplitude excitation loop. Concerning this, one may observe that excitable systems are extremely sensitive to influence of noise.

Let us consider activation process – occurrence of excitation loop (spike) in one Fitzhugh-Nagumo (FHN) element and in two coupled excitable FHN elements which are under the influence of two independent noise sources. FHN model is a canonical model for excitable systems of class II, with almost uninterrupted transitions between the small-amplitude and large-amplitude excitation loop.

We start for the following equations which describe the dynamics of an excitable unit:

$$dx = f_x(x,y) = \left[x - \frac{x^3}{3} - y\right] dt + \sqrt{2D_1} dW_1$$

$$dy = f_y(x,y) = \varepsilon(x+b)dt + \sqrt{2D_2} dW_2 \qquad (23)$$

Model (23) is typical for excitable systems of class II, which means that the position of equilibrium is near the direct supercritical Hopf bifurcation. Parameter b directly determines the possible occurrence of bifurcation. Critical value of parameter b is $|b| = 1$, since for higher values system is in the state of stable equilibrium, while oscillations occur for lower values. Due to the symmetry of the system (23), analysis could be conducted for b>0 without the loss of generality. System (23) exhibits the excitable behavior if the value of parameter b is near the bifurcation value (1.05).

Next important property of model (23) is the clear distinction between the activation variable and recovery variable, which is achieved by small value of parameter ε (0.05).

In (23) influence of noise is represented by Wiener processes, for which $\langle dWi \rangle = 0$ and $\langle dWidWj \rangle = dt\delta_{ij}$, i,j=1,2, stand. Excitable unit is in the equilibrium state in the absence of perturbation. Effect of perturbation could lead to small deviation from equilibrium state, which is followed by the fast return to equilibrium state, or to large loop followed by the return in equilibrium state only after the whole oscillation cycle is finished.

For the sake of further analysis, it is important to consider the geometric interpretation of the system (23). Two important questions arise: (1) existence and structure of the boundary between initial conditions which lead to small or large deviation from equilibrium state; (2) difference between $D_1$ and $D_2$ which cause large loop from equilibrium state.

Regarding the first question, by using perturbation theory, let us analyze the deterministic nature (without the noise) of the system (23), which for ε→0 turns to one-dimensional system $\dot{x} = f_x(x, y)$ for which $\dot{y} = 0$ stands, which means that y, instead of variable, becomes the fixed parameter. For small but finite $\varepsilon$, $x$ reaches quickly to value that is given by the equation $f_x(x,y) = 0$, e.g., to curve which is called $x$ (cube) nullcline. This nullcline consists of three branches: refractory branch $S_R$, spiking branch $S_S$, which we could consider as attractors when ε→0 and the middle branch which is unstable and which is the part of separatrix between the branches-attractors. It is important to emphasize that for small but finite ε, structure of the boundary between two areas and the corresponding threshold behavior is highly affected by the singular boundary when ε→0. Small but finite ε causes the foliation of the boundary near the maximum of $x$-nullcline. By using the "blow-up" method (Krupa and Szmolyan, 2001) one can show that the boundary between initial conditions which lead to branch Ss or $S_R$ is not the simple line, but thin layer composed of inifinite family of the trajectories of system (23), which means that the boundary represents invariant set. This boundary could still be considered as a simple line, "ghost separatrix" (Khovanov et al., 2013), since at the distance d >> ε from the fold point (1,2/3) trajectories which compose the boundary could be hardly recognized one from another.

It is clear that when the noise is included in the dynamics of slow variable, it could move the position of the y-nullcline. In other words, internal noise could translatory move the fixed point from stable refractory branch to unstable (middle) branch of the x-nullcline, which further temporarily brings

the system for excitable to oscillatory state. Impact of $D_2$ could be understood by geometric analysis, which is not the case for the impact of $D_1$.

Let us now consider the statistics of the activation events, which is characterized by TFP$\tau(D_1,D_2)$, where TFP stands for Time-to-First-Pulse, and by the variation coefficient $R(D_1,D_2)$. TFP represents the average value of TFPs obtained for different stochastic realizations:

$$\tau(D_1, D_2) = \frac{1}{n_r}\sum_{i=1}^{nr} \tau_i(D_1, D_2) \tag{24}$$

Trajectories that are taken into consideration fulfill the previous boundary conditions, e.g., they start from the fixed point and come to the spiking branch of the cube nullcline. Variation coefficient is defined in the following way:

$$R(D_1, D_2) = \frac{\sqrt{\langle \tau_i^2 \rangle - \langle \tau_i \rangle^2}}{\langle \tau_i \rangle} \tag{25}$$

where $\langle \cdot \rangle$ denotes the averaging over the ansamble of stochastic realizations. Coefficient R describes the regularity of the activation process, such that smaller R indicates the individual values of TFP are with smaller deviation from the average values. We use Oyler integration method with fixed time step $\delta t = 0.002$. Average values of TFP are obtained by averaging over 5000 different stochastic realizations of the activation process.

As shown in Franović et al., (2015), average value of TFP is strongly dependent on $D_1$, while R depends on $D_2$. Also, one can make a difference among three characteristic regimes of the average TFP: (i) long TFP, for small $D_1$ and $D_2$, (ii) plateaum for average values of $D_1$ and average to high values of $D_2$, and (iii) short TFP, for high values of $D_1$, independently of the value of $D_2$. Boundaries between these regimes, naturally, due to the effect of noise are not sharp, but gradual.

It is important to emphasize that transitions between regimes (i) and (ii) could be qualitatively explained by the existence of stochastic bifurcation of the excitable unit, induced by the influence of $D_1$ and $D_2$. This bifurcation actually represents the phenomenological stochastic bifurcation which corresponds to the transition from the position of the stochastically stable fixed point to stochastically stable limit cycle [Arnold, 1999; Acebron et al., 2004; Gaudreault et al., 2009; Gaudreault et al., 2011]. Fixed point could be considered stochastically stable if the amplitude of fluctuations around the

fixed point is the same order of unit as the noise intensity, while, on the other hand, stochastic limit cycle could be considered stochastically stable if the structure that includes two branches of the x nullcline (spiking and refractory branch) remains preserved when effect of noise is considered.

Before the stochastic bifurcation, average value of TFP is higher, and after the bifurcation induced by noise average value of TFP significantly decreases, and, in significant portion, no longer depends on the further increase of noise intensity. In other words, when fixed point becomes stochastically unstable, impact of noise is constant regardless of the intensity since the strength of the attraction of the fixed point is no longer sufficient to resist the impact of noise.

Boundary between the areas with higher values of TFP and plateau aligns with the set of values ($D_1$,$D_2$) for which stochastic bifurcation arises. This set of values ($D_1$,$D_2$) is determined analytically in a way that one needs previpusly to formulate a deterministic models using the Gaussian approximation of the starting system (23). In accordance to Gaussian approximation all cummulants above the second order are equal to zero (Tanabe and Pakdaman, 2001; Franović et al., 2013; Burić et al., 2010), when one arrives at the set of five equations which describe dynamics of the first moments, $m_x(t) = E[x(t)]$ and $m_y = E[y(t)]$, variances $Sx(t) = E([x(t)-m_x(t)]^2$ and $S_y(t) = E([y(t)-m_y(t)]^2$, and the covariance $U(t) = E([x(t)-m_x(t)][y(t)-m_y(t)]$:

$$\dot{m}_x = m_x - \frac{1}{3}m_x^3 - m_x s_x - m_y$$

$$\dot{m}_y = \varepsilon(m_x + b)$$

$$\dot{s}_x = 2s_x(1 - m_x^2 - s_x) - 2U + 2D_1$$

$$\dot{s}_y = 2\varepsilon U + 2D_2$$

$$\dot{U} = U(1 - m_x^2 - s_x) + \varepsilon s_x - s_y \qquad (26)$$

Impact of noise in (26) is included with the parameters $D_1$ and $D_2$, wich could be considered as bifurcation parameters. Bifurcation analysis shows that system (26) goes through supercritical Hopf bifurcation which enables to understand the transition between regime (i) and (ii) in the starting system (23). Bifurcation curve $D_2(D_1)$ qualitatively characterizes the stochastic bifurcation of the excitable unit, and which is revealed in the transition

between areas with high and moderate values of TFP and areas with plateau of average values of TFP.

## Conclusion

Present chapter deals with the noise recorded in real conditions in the Earth's crust and methods for the analysis of the noise. In particular, we examined the effect of random and colored noise on the onset of seismogenic fault motion, and the rôle fo random noise in groundwater level dynamics. For this purpose, we introduce the mean-field approach, which enable derivation of deterministic system with qualitatively the same behavior as the starting stochastic system.

This chapter represents the retrospective of the authors' work, since it is mainly based on the previous studies by Kostić et al., (2017, 2019, 2020), and Vasović et al., (2016).

In the first part of the chapter we introduce the mean-field approach for the analysis of the stochastic differential equations with time delay. We present the main idea, proofs for the validity, as well as conditions for which the proposed MFA approach fails.

In the second part of the chapter, we examine the effect of random noise on the earthquake nucleation process. In particular, we examine dynamics of the sprin-block model comprised of 100 blocks, using the proposed MFA approach, by which we reduced the starting system to five delay differential equations, which exhibit qualitatively similar dynamics as the starting stochastic system. Introduction of random noise is corroborated by the results of nonlinear time series analysis of the real observed movement along the Sand Andreas fault. Time delay is explicitly introduced in correspondence to the original idea of Burridge and Knopoff (1967). Result sobtainedindicate the occurrence of long-period aperiodic irregular oscillations due to the effect of random noise or under the impact of global attractor. One should note that delayed interaction among different parts of the fault, including the background seismic noise is for the first time analyzed by the authors of this chapter. Moreover, it is shown that the sole effect of seismic noise or the influence of seismic noise in the presence of local and global attractor could lead to the transition from equilibrium state to aseismic creep – these irregular oscillations are shown to obey power-law behavior.

In the third part of the chapter, we analyze the effect of random noise on the onset of seismogenic fault motion in case of varying neighboring

interactions. Sarting from the original system of *2N* coupled stochastic delay-differential equations, using MFA approach we have derived a system comprised of only of two deterministic delay-differential equations for the approximate system. Results of our analysis indicate the predominant influence of delayed interaction, which is found to strongly depend on the coupling strength and friction. For the case of weak coupling and also low friction, delayed interaction does not have any impact on destabilization of fault motion. Regarding the effect of seismic noise, which is of primary interest in this chapter is not dominant, especially for the values which are justified, when compared to the real observed data (ratio of seismic noise to velocity should be smaller than $10^{-2}$). On the other hand, the effect of strong seismic noise (e.g., $D \approx 1.0$) is similar to the influence of high values of friction and coupling strength: there is a certain threshold of coupling strength above which the system exhibit Andronov-Hopf bifurcation by increasing the coupling delay.

The fourth part of the chapter is devoted to the analysis of colord noise on the seismogenic fault motion. Presence of colored noise is proved by the analysis of real recorded data: strike-slip fault movement directly measured at the two points in Driny cave, Male´ Karpaty mts in Slovakia; (2) ambiental noise measurements before and after the earthquake on 8th September 2015 at the BKS station (Byerly Seismogrpahic Vault, Berkley). There are three different dynamical regimes, corresponding to the real observed regimes of fault motion: (1) steady stationary state; (2) creep regime and (3) active seismogenic motion. Rather interesting effect of correlation time and coupling strength on the earthquake nucleation process is captured. Apparently, there is no seismic motion for the higher values of correlation time and higher values of coupling strength. The difference between the effect of random and colored noise on the seimogenic fault motion is the following. Under the effect of random background noise seismic fault motion occurs only in a bi-stable dynamical regime in the vicinity of a bifurcation curve if initial conditions are far from the equilibrium state, while the effect of colored noise brings with small correlation time is crucial for the rise of seismic fault motion, under the conditions that delayed interaction is assumed.

In the fifth part of the chapter, we examine the role of noise in groundwater level dynamics. It is shown that stochasticity in the examined recorded GWL time series is significant, and it rises with the reduction of the harmonics in the proposed model. Solutions of the proposed model are given in a form of irregular time series which qualitatively resembles the real observed dynamics of groundwater level. Apart from this, we suggest the

application of the proposed stochastic model, by introduction into the existing model of landslide dynamics. Numerical bifurcation analysis of such system indicates the predominant influence of the introduced colored noise, which solely could lead to transition between different dynamical regimes, especially pronounced in case when oscillations are assumed in the starting system (landslide with long creep continuous movements).

Sixth part of the chapter is devoted to role of noise in triggering the activation process in excitable systems. In particular, we examine dynamics of Fitzhugh-Nagumo neurons, under the impact of multiple noise sources. It is shown that introduction of noise in the dynamics of slow variable induces the movement of the fixed point from stable refractory branch to unstable (middle) branch of the x-nullcline, which further temporarily brings the system for excitable to oscillatory state. Moreover, it is hown that average value of time to first pulse (TFP) depneds on the noise intensity D1, while variation coefficient R depends on the noise intensity D2. Actually, results obtained indicate three characteristic regimes of the average TFP: (1) long TFP, for small $D_1$ and $D_2$, (2) plateaum for average values of $D_1$ and average to high values of $D_2$, and (3) short TFP, for high values of $D_1$, independently from the value of $D_2$, with gradual boundaries between these regimes, due to the effect of noise. Bifurcation curve $D_2(D_1)$ qualitatively characterizes the stochastic bifurcation of the excitable unit, and which is revealed in the transition between areas with high and moderate values of TFP and areas with plateau of average values of TFP.

One should note that the presented results enable future studies in the following directions. Since it is shown that both random and colored noise exist in the real observed data and that effect of noise could have a predominant rôle in triggering the earthquake nucleation process, complex groundwater level dynamics and slope instability, use and further analysis of stochastic model sis justified and obligatory. Further analysis of such model could focus on the comparison of individual and collective behavior, or the spatial interaction among the blocks in the system. Additionaly, one could introduce a more complex friction in the analyzed system, e.g., by including the effect of the state variable. Moreover, analysis of dynamics of spring-block models could further include the case when interactions between the neighboring blocks weakens with the distance, which is for sure the more realistic scenario. As for the groundwater level dynamics, further research could include a detailed bifurcation analysis of the dynamics of the suggested model, which could shown transition between different dynamical régimes,

which is also an idea for the landslide model with included effect of GWL dynamics.

## Acknowledgments

This chapter was inspired by the work of late prof. Nikola Burić, who left invaluable results in nonlinear dynamics, primarily in the area of noise analysis and the corresponding effects on neural interactions.

## References

Acebrón, J. A., Bulsara, A. R., Rappel, W. J. 2004. "Noisy FitzHugh-Nagumo model: From single elements to globally coupled networks." *Physical Review E* 69: 026202.

Adamowski, J., Chan, H. F. 2011. "A wavelet neural network conjuction model for groundwater level forecasting." *Journal of Hydrology* 407: 28-40.

Arnold, L. 1999. *Random Dynamical Systems*, Springer, Berlin.

Boese, C., Wotherspoon, L., Alvarez, M., and Malin, P. 2015. "Analysis of anthropogenic and natural noise from multilevel borehole seismometers in an urban environment." Auckland, New Zealand. *Bulletin of the Seismological Society of America* 105(1): 285–299.

Burić, N., Ranković, D., Todorović, K., Vasović, N. 2010. "Mean-field approximation for noisy delay coupled exciateble neurons." *Physica A* 389: 3956-3964.

Burridge, R., Knopoff, L. 1967. "Model and theoretical seismicity." *Bulletin of the Seismological Society of America* 57: 341-71.

Cessaro, R. K. 1994. "Sources of primary and secondary microseisms." *Bulletin of the Seismological Society of America* 84 (1): 142 – 148.

Dodla, R., Sen, A., Johnston, G. L. 2004. "Phase-locked patterns and amplitude death in a ring of delay-coupled limit cycle oscillators." *Physical Review Letters* 69: 0562172.

Fallah-Mehdipour, E., Haddad, O. B., Marino, M. A. 2013. "Prediction and simulation of monthly groundwater levels by genetic programming." *Journal of Hydro-environment Research* 7: 253-260.

Franović, I., Todorović, K., Vasović, N., Burić, N. 2013. "Mean-field approximation of two coupled populations of excitable units." *Physical Review E* 87: 012922.

Franović, I., Todorović, K., Vasović, N, Burić, N. 2014. "Persistence and failure of mean-field approximations adapted to a class of systems of delay-coupled excitable units." *Physical Review E* 89: 022926.

Franović, I., Todorović, K., Perc, M., Vasović, N., Burić, N. 2015. "Activation process in excitable systems with multiple noise sources: One and two interacting units." *Physical review E* 92: 062911.

Fyen, J. 1990. "Diurnal and seasonal variations in the microseismic noise obsrved at the NORESS array." *Physics of the Earth and Planetary Interiors* 63: 252-268.

Gardiner, C. W. 1985. *Handbook of Stochastic Methods*. Springer, Berlin.

Gaudreault, M., Berbert, J. M., Viñals, J. 2011. "Correlation times in stochastic equations with delayed feedback and multiplicative noise." *Physical Review E* 83: 011903.

Gaudreault, M., Lépine, F., Viñals, J. 2009. "Pitchfork and Hopf bifurcation thresholds in stochastic equations with delayed feedback." *Physical Review E* 80: 061920.

Hasegawa, H. 2004. "Augmented moment method for stochastic ensembles with delayed couplings. I. Langevin model." *Physical Review E* 70: 021911.

Hong, Y. M. 2017. "Feasibility of using artificial neural networks to forecast groundwater levels in real time." *Landslides* 14: 1815-1826.

Khovanov, I. A., Polovinkin, A. V., Luchinsky, D. G., McClintock, P. V. E. 2013. "Noise-induced escape in an excitable system." *Physical Review E* 87: 032116.

Kostić, S., Vasović, N., Franović, I., Todorović, K., Klinshov, V., Nekorkin, V. 2017. "Dynamics of fault motion in a stochastic spring-slider model with varying neighboring interactions and time-delayed coupling." *Nonlinear Dynamics* 87: 2563-2575.

Kostić S., Vasović, N., Todorović, K., Franović, I. 2020. "Effect of colored noise on the generation of seismic fault movement: Analogy with spring-block model dynamics." *Chaos, Solitons & Fractals* 135: 109726.

Krupa, M., Szmolyan, P. 2001. "Extending Geometric Singular Perturbation Theory to Nonhyperbolic Points---Fold and Canard Points in Two Dimensions." *SIAM Journal on Mathematical Analysis* 33: 210.1137/S0036141099360919.

Loader C. 1999. *Local Regression and Likelihood – Statisting and Computing*. Springer. Muray Hill. USA.

McNamara, D., Ringler, A., Hutt, C., and Gee, L. 2011. "Seismically observed seiching in the Panama Canal." *Journal of Geophysical Research: Solid Earth* 116(B4).

Morales, J. E., James, G., Tonnelier, A. 2017. "Traveling waves in a spring-block chain sliding down a slope." *Physical Review E* 96: 012227.

Murphy, A. J., Savino, J. R. 1975. "A comprehensive study of long period (20-200 s) Earth noise at the high gain worldwide seismograph stations." *Bulletin of the Seismological Society of America* 65: 1827-1862.

Nakata, N., Gualtieri, L., Fichtner, A. 2019. *Seismic ambient noise*. Cambridge University Press.

Perc, M., Rupnik, M., Gosak, M., Marhl, M. 2009. "Prevalence of stochasticity in experimentally observed responses of pancreatic acinar cells to acetylcholine." *Chaos* 19: 037113-1–037113-6.

Ramana Reddy. D. V., Sen, A., Johnstonm G. I. 1998. "Time delay induced death in coupld limit cycle oscillators." *Physical Review Letters* 80: 5109-5112.

Ryabov V. B., Correig A. M., Urquizu M., Zaikin A. A. 2003. "Microseism oscillations: from deterministic to noise-driven models." *Chaos, Solitons & Fractals* 16: 195-210.

Sahoo, S., Madan, J. K. 2013. "Groundwater-level prediction using multiple linear regression and artificial neural network techniques: a comparative assessment." *Hydrogeology Journal* 21: 1865-1887.

Sanders C. O. 1993. "Interaction of the San Jacinto and San Andreas fault zones, southern California: triggered earthquake migration and coupled recurrence intervals." *Science* 260: 973-976.

Sethia, G. C., Sen, A., Atay, F. 2008. "Clustered chimera states in delay-coupled oscillator systems." *Physical Review Letters* 100: 144102.

Sreekanth, P. D., Sreedevi, P. D., Ahmed, S., Geethanjali, N. 2011. "Comparison of FFNN and ANFIS models for estimating groundwater level." *Environmental Earth Sciences* 62: 1301-1310.

Suryanarayana, Ch., Sudheer, Ch., Mahammood, V., Panigrahi, B. K. 2014. "An integrated wavelet-support vector machine for groundwater level prediction in Visakhapatnam, India." *Neurocomputing* 145: 324-335.

Tanabe, S., Pakdaman, K. 2001. "Noise-enhanced neuronal reliability." *Physical Review E* 64: 041904.

Telford W. M., Geldart L. P., Sheriff R. E. 1990. *Applied Geophysics.* 2nd ed. Cambridge: Cambridge University Press.

Vasović N., Kostić S., Franović I., Todorović K. 2016. "Earthquake nucleation in a stochastic fault model of globally coupled units with interaction delays." *Communication in Nonlinear Science and Numerical Simulation* 38: 117-129.

Webb, Spahr C. 2002. "Seismic noise on land and on the sea floor." In *International Handbook of earthquake and engineering seismology*, edited by Willian H. K. Lee, Paul Jennings, Carl Kisslinger, Hiroo Kanamori, 305-318. Elsevier.

Webb, Spahr C. 1988. "Long period acoustic and seismic measurement and ocean floor currents." *IEEE Journal of Ocean Engineering* 13 (4): 263-270.

Wilmore, P. L. 1979. "Manual of Seismological Observatory Practice." *World Data Center,* report SE-20. US Department of Commerce, NOAA, Boulder, CO.

Zaks, M. A., Sailer, X., Schimansky-Geier, L., Neiman, A. B. 2005. "Noise induced complexity: From subthreshold oscillations to spiking in coupled excitable systems." *Chaos* 15: 2005, 026117.

# Index

## G



## H



## I



## L



## M



## N



## O

## P



## Q



## R



## S



## T



## V



## W

Victoria M. Petrova
Editor

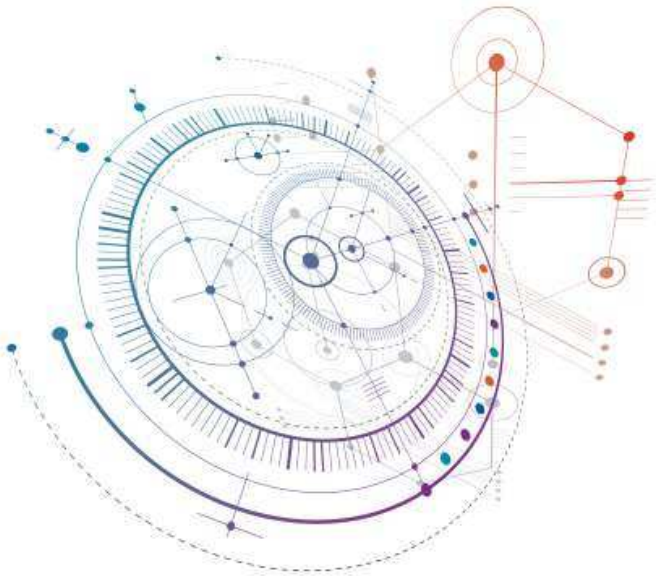

# Advances in Engineering Research

Volume 50

nova
science publishers
www.novapublishers.com

ISBN-13: 979-8-88697-353-2
9 798886 973532